Electronic Supplementary Information

Luminescent Carbene-Copper(I)-Amide Polymers for Efficient Host-Free Solution-Processed OLEDs

Yao Tan, Ao Ying, Jianlong Xie, Guohua Xie and Shaolong Gong*

College of Chemistry and Molecular Sciences, Hubei Key Lab on Organic and Polymeric Optoelectronic Materials, Wuhan University, Wuhan 430072, China.

E-mail: slgong@whu.edu.cn

General information

All reagents were used as received from commercial sources unless otherwise stated. Tetrahydrofuran and toluene were dried by sodium-potassium alloy. ^{1}H NMR and ^{13}C NMR spectra were measured on a Bruker Advanced II (400 MHz) spectrometer. High-resolution mass spectra (HRMS) were measured on a LCQ-Orbitrap Elite (Thermo-Fisher Scientific, Waltham, MA, USA) mass spectrometer. The number (M_n) and weight (M_w) average molecular weight, and polydispersity index (PDI) were determined by a Waters 2695 GPC system, using THF as the eluent (1.0 mL min^{-1}). Root-mean-square roughness of surface in neat films were measured by a SPM-9700HT atomic force microscope. The content of Cu element in the Cu(I) polymers were determined by an inductively coupled plasma-atomic emission spectroscopy (Agilent 5110).

Theoretical calculation

Density functional theory (DFT) and time-dependent DFT (TD-DFT) simulations were performed using Gaussian 16 programs. Ground state structures and FMOs were obtained by B3LYP density functional method with basis set def2-SVP. The dispersion correction was conducted by Grimme's D3 version.[1,2] Time-dependent DFT with PBE0 functional and basis set def2-SVP were then performed to further analyze the excited states with the optimized ground state structures.[3]

Photophysical characterization

Thin films for photophysical characterization were prepared by spin-coating on quartz substrates using 10 mg mL^{-1} chlorobenzene solution. Absorption spectra were characterized by a UV-visible spectrophotometer (UV-2700, Shimadzu). Photoluminescence (PL) and phosphorescence spectra were characterized by a spectrofluorimeter (F-4600, Hitachi Inc.). Phosphorescence spectra of thin films were measured at 77 K (the liquid nitrogen temperature). Absolute photoluminescence quantum efficiencies (Φ_{PL}) of these polymers in neat films were determined using a Hamamatsu's established C9920-02 measurement system (Hamamatsu Photonics) equipped with a calibrated integrating sphere, a xenon lamp, and a model C10027-01 photonic multichannel analyzer. During the Φ_{PL} measurements, the integrating sphere was purged with pure and dry nitrogen to keep the environment inert. The selected monochromatic excitation light was used to excite samples placed in the calibrated integrating sphere. Time-resolved PL (PL decay curves) was measured by monitoring the decay of the intensity at the PL peak wavelength using a FluoTime 300 Spectrometer (PicoQuant) with a Picosecond Pulsed UV-LASTER (LASTER375) as the excitation source. No light filter was used. For temperature-dependent spectra and TRPL measurements, the samples were placed in a vacuum cryostat chamber with a temperature control. The solution samples were bubbled with argon for 20 minutes before TRPL measurement.

Quantitative analyses of the corresponding rate constants

Temperature-dependent lifetimes were fitted by Boltzmann type equation (eq. S1), where $k_{r,S}$ and $k_{r,T}$ are the rate constants for radiative decay from the S_1 and T_1 states, respectively, K_B is Boltzmann's constant, and T is temperature.[4]

$$\tau = \frac{3+\exp(-\frac{\Delta E_{ST}}{k_B T})}{3k_{r,T}+k_{r,S}\exp(-\frac{\Delta E_{ST}}{k_B T})} \qquad \text{(S1)}$$

The ΔE_{ST}s were calculated by Arrhenius plot (eq. S2), where k_{ISC} and k_{RISC} represent the intersystem crossing (ISC) rate constant, the reverse intersystem crossing (RISC) rate constant, respectively. Based on eq. S2, the Arrhenius plot shows a linear dependence of $\ln k_{TADF}$ as a function of 1/T with a slope of $\Delta E_{ST}/k_B$.[6]

$$\ln k_{TADF} = \ln\left(\frac{K_{ISC}}{3}\left(1-\frac{K_{ISC}}{K_{ff}+K_{ISC}}\right)\right) - \frac{\Delta E_{ST}}{K_B T} = \ln b - \frac{\Delta E_{ST}}{K_B T} \qquad \text{(S2)}$$

Device fabrication and measurement

The pre-patterned indium tin oxide (ITO) substrates were consecutively cleaned by acetone and ethanol in an ultrasonic bath. Afterwards, the substrates were dried with N_2 and then loaded into a UV-Ozone chamber. After UV-Ozone treatment, a layer of PEDOT:PSS was spin-coated on the ITO substrate as the hole-injecting layer, and then annealed at 120 °C for 10 min inside a N_2-filled glove-box. The neat emitter layer was spin-coated directly onto the hole-injecting layer from the chlorobenzene solvent (10 mg/mL), and then annealed at 50 °C for 10 min. Afterwards, the hole-blocking layer, the electron-transporting layer, and the cathode were consecutively thermally evaporated onto the emitter layer in a vacuum chamber. Before taken out of the glove-box, the devices were encapsulated with UV-curable epoxy. The voltage-current-luminance characteristics and the EL spectra were simultaneously measured with PR735 SpectraScan Photometer and Keithley 2400 sourcemeter unit under ambient atmosphere at room temperature.

Synthesis routes

All reagents were used as received from commercial sources unless otherwise stated. The key precursors CAAC-CuCl and MAC-CuCl were synthesized according to the reported literature procedures.[5,6]

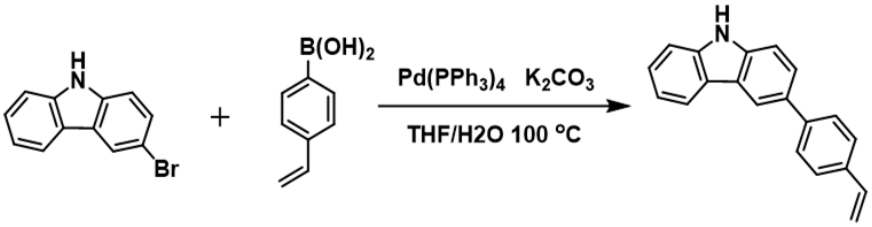

Scheme S1 Synthetic route of the donor ligand.

3-(4-vinylphenyl)-9*H*-carbazole: 3-Bromo-9*H*-carbazole (1.0 g, 4 mmol), (4-vinylphenyl)boronic acid (720 mg, 4.8 mmol), $Pd(PPh_3)_4$ (234 mg, 0.2 mmol) and K_2CO_3 (1.1 g, 8 mmol) were added to THF (12 mL) and H_2O (4 mL) mixing solutions. The reaction was stirred at 100 °C overnight. The reaction mixture was extracted with CH_2Cl_2 and washed with water. The organic phase was dried over anhydrous Na_2SO_4 and concentrated under reduced pressure. The crude product was purified by column chromatography with petroleum ether/CH_2Cl_2 (v/v = 2:1) as eluent, finally the white powder (861 mg, 3.3 mmol). Yield: 81%. ^{1}H NMR (400 MHz, $CDCl_3$+TMS, 300 K, ppm) δ = 8.15 (d, *J* = 7.7 Hz, 2H), 7.68–7.61 (m, 2H), 7.59–7.50 (m, 2H), 7.45–7.38 (m, 4H), 7.32–7.26 (m, 2H), 6.83 (dd, *J* = 17.6, 10.9 Hz, 1H), 5.86 (d, *J* = 17.6 Hz, 1H), 5.37 (d, *J* = 11.7 Hz, 1H). ^{13}C NMR (101 MHz, $CDCl_3$+TMS, 300 K, ppm) δ = 141.5, 140.0, 139.0, 136.6, 135.8, 132.6, 127.3, 126.7, 126.1, 125.3, 124.0, 123.5, 120.4, 119.7, 118.7, 113.5, 110.8, 110.8.

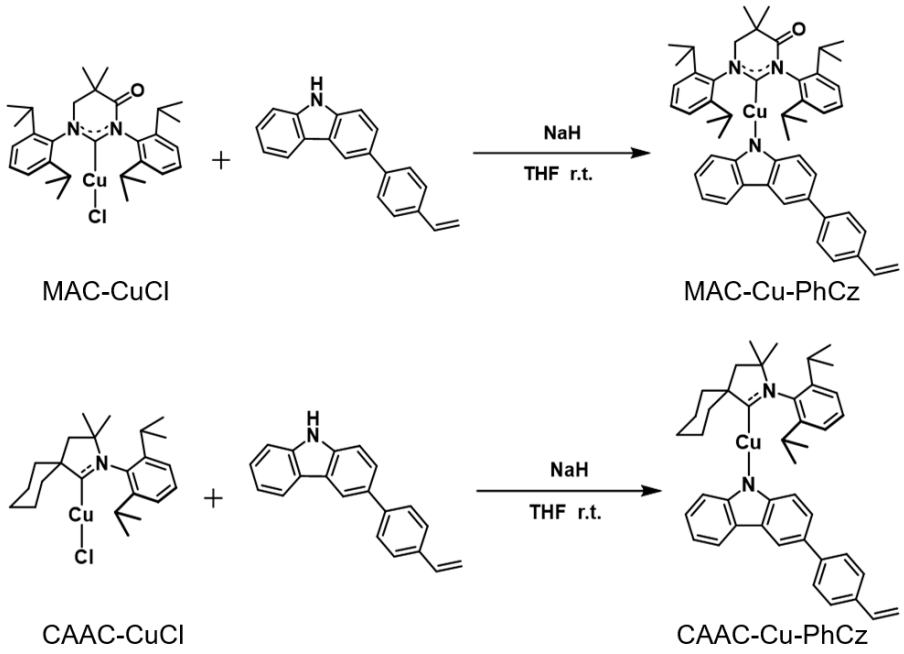

Scheme S2 Synthetic routes of the Cu(I)-CMA monomers.

MAC-Cu-PhCz monomer: 3-(4-Vinylphenyl)-9*H*-carbazole (511 mg, 1.9 mmol) and NaH (54 mg, 2.3 mmol) were dissolved in 10 mL THF and stirred at 0.5 h at 40 °C. MAC-CuCl (1.0 g, 1.9 mmol) was added to the reaction and stirred for 3 h. the resulting mixture was filtered through Celite, and the solvent was removed under reduced pressure to afford a yellow solid. The rude solid was redissolved in dry CH_2Cl_2, and dry hexane was added to precipitate the pure product (1.1 g, 1.4 mmol). Yield: 74%.

^{1}H NMR (400 MHz, CD_2Cl_2+TMS, 300 K, ppm) δ = 7.98 (s, 1H), 7.74 (d, *J* = 6.9 Hz, 1H), 7.67 (td, *J* = 7.8, 5.4 Hz, 2H), 7.54 (d, *J* = 8.3 Hz, 2H), 7.48–7.32 (m, 6H), 7.09 (dd, *J* = 8.5, 2.0 Hz, 1H), 6.84–6.77 (m, 1H), 6.76–6.70 (m, 1H), 6.70–6.63 (m, 1H), 5.69 (d, *J* = 17.6 Hz, 1H), 5.46–5.39 (m, 2H), 5.13 (d, *J* = 11.8 Hz, 1H), 3.84 (s, 2H), 3.26 (m, 2H), 3.02 (m, 2H), 1.53(s, 8 Hz), 1.34 (d, *J* = 6.8 Hz, 6H), 1.18 (t, *J* = 6.9 Hz, 16H). ^{13}C NMR (101 MHz, CD_2Cl_2+TMS, 300 K, ppm) δ = 210.4, 171.1, 150.4, 149.5, 146.3, 145.3, 142.7, 140.1, 136.7, 136.0, 134.6, 130.6, 130.3, 127.6, 126.6, 126.4, 125.8, 125.0, 124.3, 124.0, 123.3, 122.3, 118.9, 117.1, 115.6, 114.7, 114.7, 112.3, 61.9, 38.0, 29.2, 28.9, 24.1, 23.9, 23.8. Elemental analysis calcd. for $C_{50}H_{56}N_3OCu$: C, 77.18%; H, 7.20%; N, 5.40%. Found: C, 76.98%; H, 7.31%; N, 5.28%.

CAAC-Cu-PhCz monomer: 3-(4-Vinylphenyl)-*9H*-carbazole (511 mg, 1.9 mmol) and NaH (54 mg, 2.3 mmol) were dissolved in 10 mL THF and stirred at 0.5 h at 40 °C. CAAC-CuCl (806 mg, 1.9 mmol) was added to the reaction and stirred for 3 h. The resulting mixture was filtered through Celite, and the solvent was removed under reduced pressure to afford a white solid. The rude solid was redissolved in dry CH_2Cl_2, and dry hexane was added to precipitate the pure product (1.0 g, 1.6 mmol). Yield: 83%. ^{1}H NMR (400 MHz, CD_2Cl_2+TMS, 300 K, ppm) δ = 8.23 (d, *J* = 1.9 Hz, 1H), 8.01 (d, *J* = 7.6 Hz, 1H), 7.78–7.66 (m, 3H), 7.52 (dd, *J* = 8.0, 2.9 Hz, 4H), 7.42 (dd, *J* = 8.5, 2.0 Hz, 1H), 7.15 (t, *J* = 8.2 Hz, 1H), 6.97 (t, *J* = 7.0 Hz, 1H), 6.88–6.75 (m, 2H), 6.67 (d, *J* = 8.5 Hz, 1H), 5.82 (d, *J* = 18.6 Hz, 1H), 5.27 (d, *J* = 11.5 Hz, 1H), 3.03 (hept, *J* = 6.8 Hz, 2H), 2.49–2.33 (m, 2H), 2.24 (s, 2H), 2.11 (m, 2H), 1.91 (m, 1H), 1.83–1.62 (m, 5H), 1.50 (s, 6H), 1.39 (d, *J* = 6.8 Hz, 6H), 1.27 (d, *J* = 6.7 Hz, 6H). ^{13}C NMR (101 MHz, CD_2Cl_2+TMS, 300 K, ppm) δ = 250.5, 150.6, 149.7, 145.8, 142.7, 136.7, 135.3, 134.7, 129.7, 127.7, 126.6, 126.5, 125.2, 124.6, 124.4, 123.6, 122.6, 119.3, 117.4, 115.7, 114.7, 114.7, 112.4, 80.5, 59.4, 46.4, 36.7, 29.5, 29.2, 26.4, 25.7, 22.4, 22.3. Elemental analysis calcd. for $C_{43}H_{49}NCu$: C, 78.75%; H, 7.48%; N, 4.27%. Found: C, 78.62%; H, 7.64%; N, 4.07%.

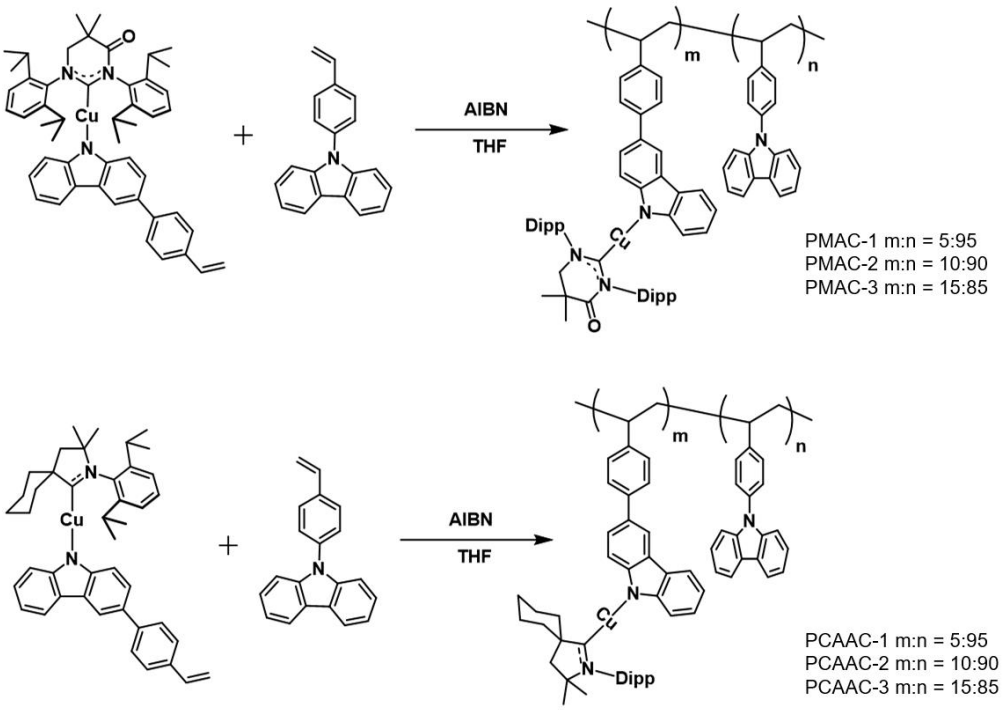

Scheme S3 Synthetic routes of the Cu(I) polymers.

Synthetic procedure of the Cu(I) polymers:

The polymers were synthesized by free radical polymerization with azodiisobutyronitrile (AIBN) as the radical initiator and THF as the solvent. The Cu(I)-CMA complexes monomers and AIBN (1% of the total amount of the monomers) were dissolved in THF at 50 °C for 48 h under nitrogen atmosphere. After cooling to room temperature, the solvent was removed under reduced pressure to afford rude products. The rude solid were boiled in acetone for 3 h and then filtered to afford purified solid.

PMAC-1: MAC-Cu-PhCz (150 mg, 0.2 mmol), 9-(4-vinylphenyl)-9*H*-carbazole (980 mg, 3.8 mmol) and AIBN (7 mg, 0.04 mmol) were used in the free radical polymerization. Yield: 87%. ^{1}H NMR (400 MHz, CD_2Cl_2+TMS, 300 K, ppm) δ = 8.21–7.75 (bs), 7.65–6.40 (br), 3.97–3.64 (br), 3.38–2.81 (br), 2.75–1.66(br), 1.43–0.98 (br). ^{13}C NMR (101 MHz, CD_2Cl_2+TMS, 300 K, ppm) δ = 170.6, 143.9 140.4, 135.5, 129.0, 126.4, 125.7, 123.1, 120.0, 119.7, 109.3, 40.8, 37.7, 29.0, 28.7, 25.5, 24.49, 24.01, 23.75, 13.8. Elemental analysis. Found: C, 87.20%; N, 4.68%; H, 6.15%. GPC: M_n: 56.4 kDa, M_w: 116.8 kDa, PDI: 2.07.

PMAC-2: MAC-Cu-PhCz (300 mg, 0.4 mmol), 9-(4-vinylphenyl)-9*H*-carbazole (928 mg, 3.6 mmol) and AIBN (7 mg, 0.04 mmol)

were used in the free radical polymerization. Yield: 86%. ^{1}H NMR (400 MHz, CD_2Cl_2+TMS, 300 K, ppm) δ = 8.06–7.64 (bs), 7.48–6.28 (br), 3.80–3.51 (br), 3.25–2.70 (br), 2.53–1.55(br), 1.32–0.83 (br). ^{13}C NMR (101 MHz, CD_2Cl_2+TMS, 300 K, ppm) δ = 170.9, 145.5, 144.1, 140.3, 135.4, 128.9, 126.4, 125.7, 125.3, 124.9, 124.5, 123.1, 119.8, 109.3, 40.8, 37.9, 36.2, 33.5, 31.6, 29.0, 28.6, 27.0, 24.6, 24.5, 24.3, 24.0, 23.8, 23.6, 22.7, 22.6, 22.4, 18.5, 13.9, 11.2. Elemental analysis. Found: C, 86.02%; N, 4.64%; H, 6.36%. GPC: M_n: 40.2 kDa, M_w: 85.4 kDa, PDI: 2.12.

PMAC-3: MAC-Cu-PhCz (450 mg, 0.6 mmol), 9-(4-vinylphenyl)-9*H*-carbazole (876 mg, 3.6 mmol) and AIBN (7 mg, 0.04 mmol) were used in the free radical polymerization. Yield: 82%. ^{1}H NMR (400 MHz, CD_2Cl_2+TMS, 300 K, ppm) δ = 8.21–7.72 (bs), 7.49–6.43 (br), 3.9–3.63 (br), 3.38–2.83 (br), 2.59–1.67(br), 1.43–0.98 (br). ^{13}C NMR (101 MHz, CD_2Cl_2+TMS, 300 K, ppm) δ = 170.7, 145.5, 144.4, 140.4, 135.5, 129.0, 126.4, 125.7, 125.3, 124.5, 123.2, 120.0, 109.4, 40.8, 37.9, 31.6, 29.2, 29.1, 29.0, 28.6, 26.9, 24.6, 24.5, 24.3, 24.0, 23.8, 23.6, 22.7, 22.6, 22.4, 18.5, 14.0, 11.2. Elemental analysis. Found: C, 83.80%; N, 4.47%; H, 6.51%. GPC: M_n: 52.1 kDa, M_w: 114.4 kDa, PDI: 2.19.

PCAAC-1: CAAC-Cu-PhCz (131 mg, 0.2 mmol), 9-(4-vinylphenyl)-9*H*-carbazole (980 mg, 3.8 mmol) and AIBN (7 mg, 0.04 mmol) were used in the free radical polymerization. Yield: 76%. ^{1}H NMR (400 MHz, CD_2Cl_2+TMS, 300 K, ppm) δ = 8.08–7.78 (bs), 7.47–6.64 (br), 2.98–2.77 (m), 2.68–1.65 (br). ^{13}C NMR (101 MHz, CD_2Cl_2+TMS, 300 K, ppm) δ = 167.0, 146.4, 145.7, 142.2, 141.1, 136.5, 131.5, 125.1, 122.5, 121.7, 120.9, 119.2, 115.9, 111.7, 110.5, 105.5, 57.4, 36.8, 33.9, 25.0, 24.7, 20.5, 20.0, 19.78, 9.9. Elemental analysis. Found: C, 86.56%; N, 4.91%; H, 6.16%. GPC: M_n: 43.3 kDa, M_w: 90.7 kDa, PDI: 2.10.

PCAAC-2: CAAC-Cu-PhCz (262 mg, 0.4 mmol), 9-(4-vinylphenyl)-9*H*-carbazole (928 mg, 3.6 mmol) and AIBN (7 mg, 0.04 mmol) were used in the free radical polymerization. Yield: 83%. ^{1}H NMR (400 MHz, CD_2Cl_2+TMS, 300 K, ppm) δ = 8.10–7.77 (bs), 7.49–6.65 (br), 2.96–2.78 (m), 2.69–1.67 (br). ^{13}C NMR (101 MHz, CD_2Cl_2+TMS, 300 K, ppm) δ = 140.4, 135.6, 129.0, 128.2, 126.4, 125.7, 123.1, 119.9, 109.4,40.5, 36.8, 36.129.4, 29.4, 29.1, 26.3, 25.7 22.3, 16.2, 14.1. Elemental analysis. Found: C, 84.98%; N, 4.88%; H, 6.34%. GPC: M_n: 51.1 kDa, M_w: 108.1 kDa, PDI: 2.12.

PCAAC-3: CAAC-Cu-PhCz (393 mg, 0.6 mmol), 9-(4-vinylphenyl)-9*H*-carbazole (876 mg, 3.6 mmol) and AIBN (7 mg, 0.04 mmol) were used in the free radical polymerization. Yield: 81%. ^{1}H NMR (400 MHz, CD_2Cl_2+TMS, 300 K, ppm) δ = 8.15–7.78 (bs),

7.49–6.50 (br), 2.99–2.74 (m), 2.69–1.67 (br), 1.27–0.99 (br). ^{13}C NMR (101 MHz, CD_2Cl_2+TMS, 300 K, ppm) δ = 140.4, 135.6, 129.0, 128.2, 126.5, 125.7, 123.1, 120.0, 109.4, 60.3, 41.2, 36.5, 36.0, 29.4, 29.0, 26.4, 25.6, 22.3, 20.8, 14.0. Elemental analysis. Found: C, 84.28%; N, 4.85%; H, 6.55%. GPC: M_n: 29.0 kDa, M_w: 62.7 kDa, PDI: 2.16.

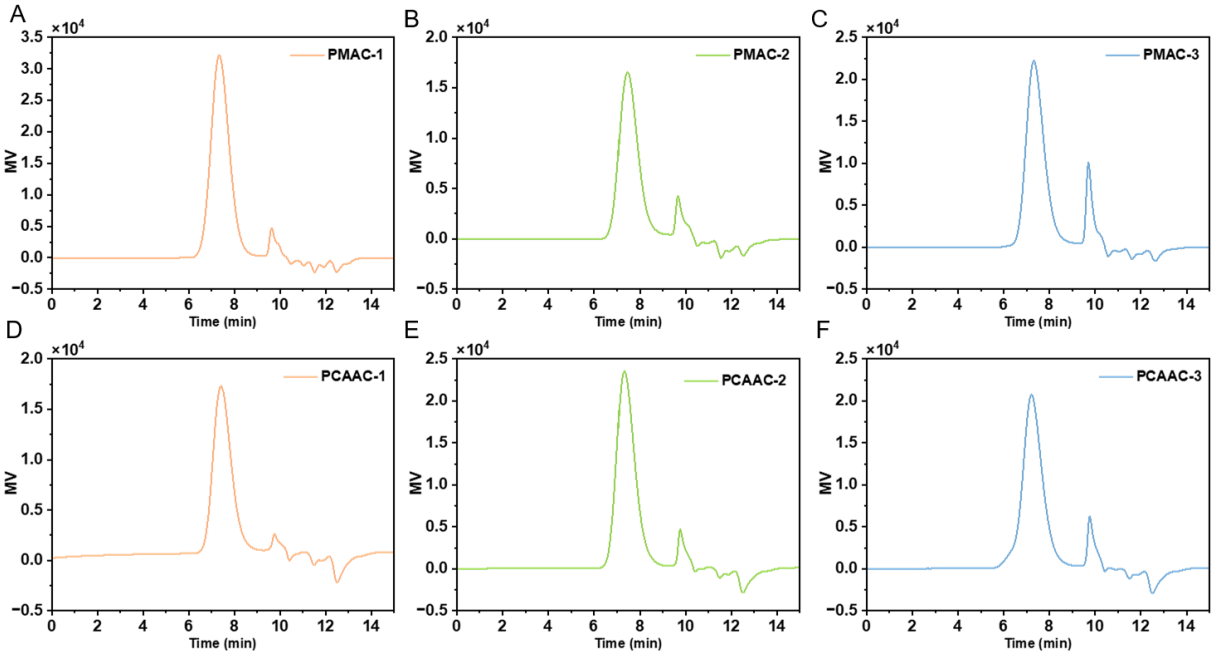

Fig. S1 GPC chromatograms of all the Cu(I) polymers.

Table S1. Characterization Data for all the Cu(I) polymers.

Polymer	M_w[a] [kDa]	PDI[a]	$Cu_{theoretical}$ [%]	Cu_{exp}[b] [%]	T_d[c] [°C]	T_g [°C]	HOMO[d] [eV]	LUMO[e] [eV]
PMAC-1	56.4	2.07	1.1	0.9	368	222	–5.26	–2.75
PMAC-2	40.2	2.12	2.0	1.8	359	227	–5.21	–2.70
PMAC-3	52.1	2.19	2.7	2.7	362	235	–5.29	–2.78
PCAAC-1	43.3	2.10	1.1	1.0	363	217	–5.41	–2.58
PCAAC-2	51.1	2.12	2.0	1.7	358	221	–5.44	–2.61
PCAAC-3	29.0	2.16	2.9	2.8	351	211	–5.41	–2.58

[a] Determined by GPC, eluting with THF, by comparison with polystyrene standard. [b] Determined by atomic emission spectroscopy. [c] Temperature at 5% weight loss. [d] Calculated from the onset oxidation potential in CH_2Cl_2 solution. [e] Calculated from HOMO and E_g (the onset of UV-visible spectra in CH_2Cl_2 solution).

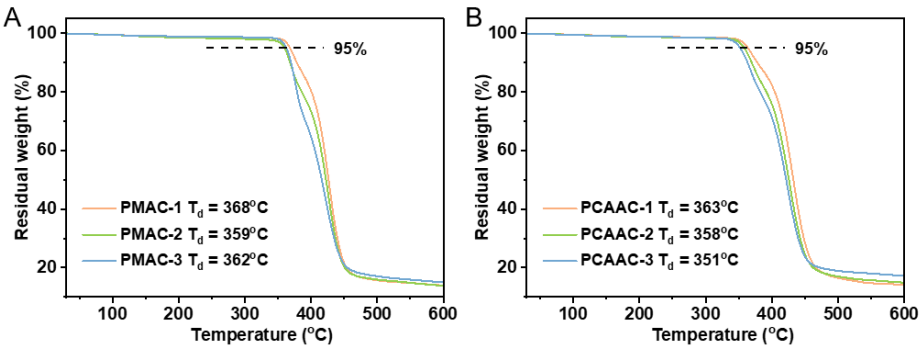

Fig. S2 TGA traces of all the Cu(I) polymers recorded at a heating rate of 10 °C min^{-1}.

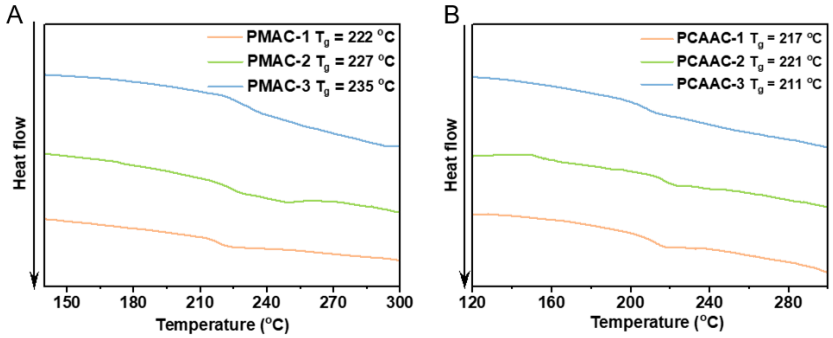

Fig. S3 DSC traces of all the Cu(I) polymers recorded at a heating rate of 10 °C min^{-1}.

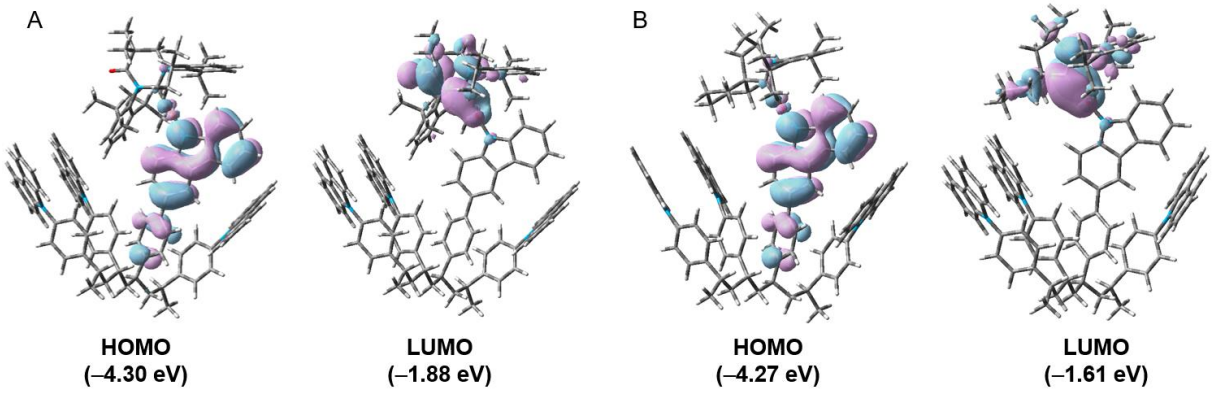

Fig. S4 Frontier molecular orbital (FMO) separation of (A) **PMAC** and (B) **PCAAC** oligomers.

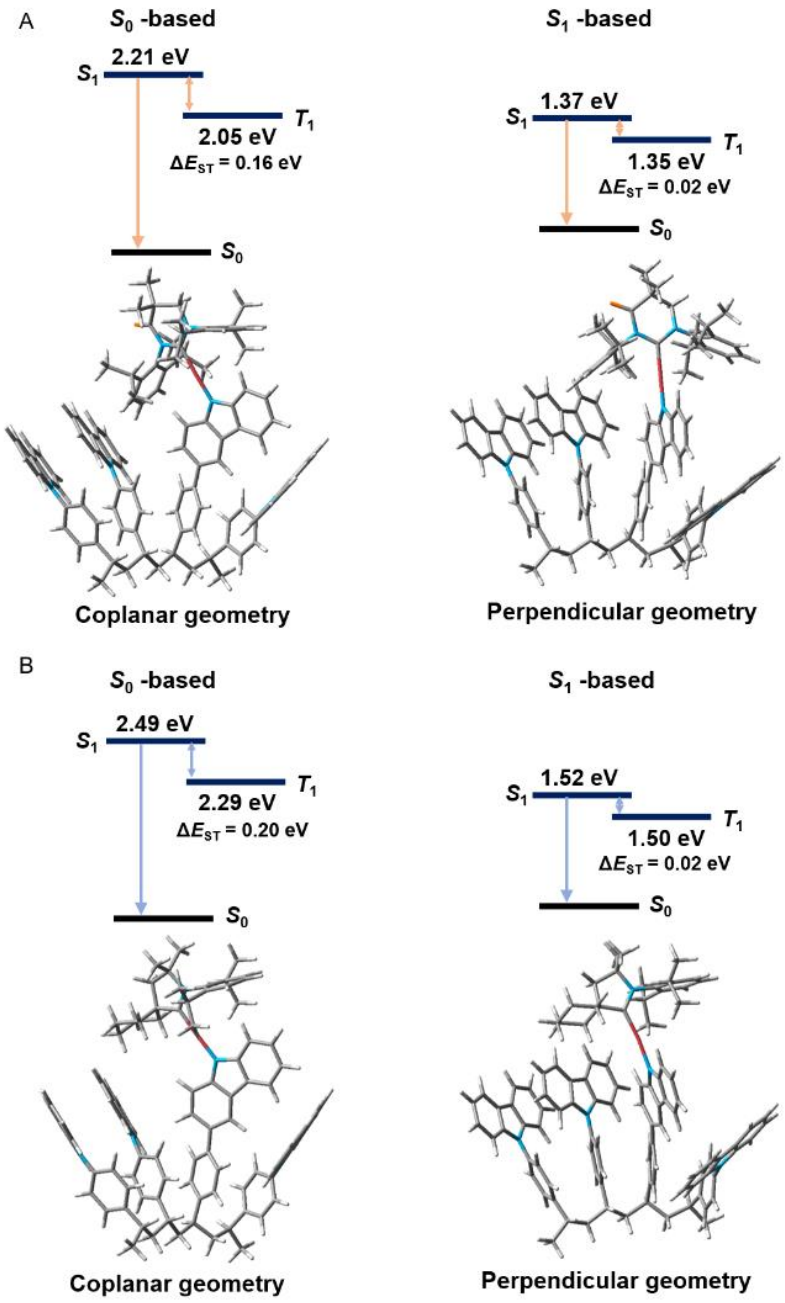

Fig. S5 Calculated energy levels with the optimized S_0 and S_1 structures of the (A) **PMAC** and (B) **PCAAC** oligomers.

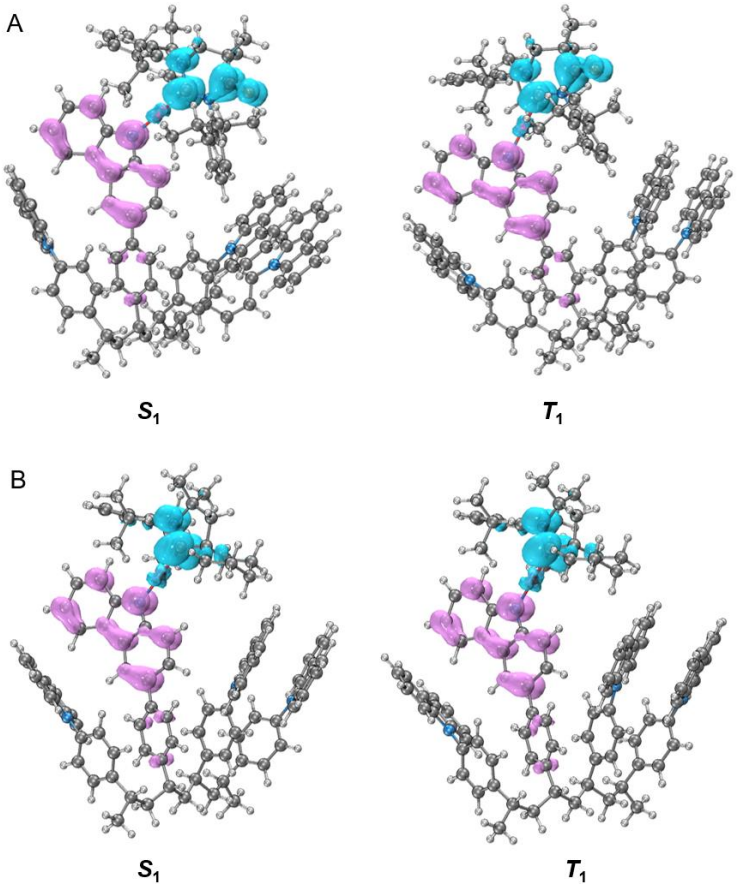

Fig. S6 hole/electron distributions of S_1 and T_1 excited states for the (A) **PMAC** and (B) **PCAAC** oligomers.

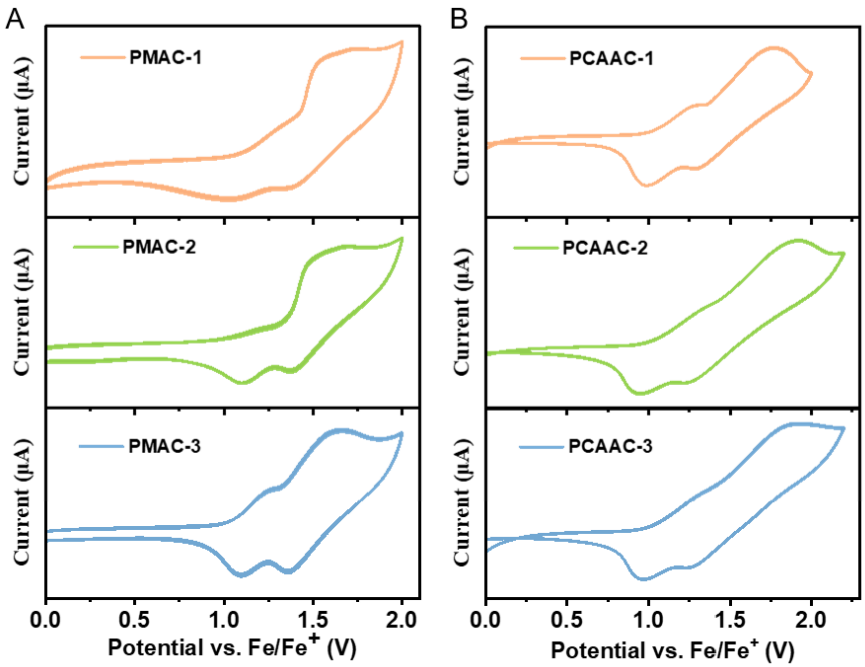

Fig. S7 Cyclic voltammograms of (A) **PMAC-x** and (B) **PCAAC-x** in CH_2Cl_2 solutions.

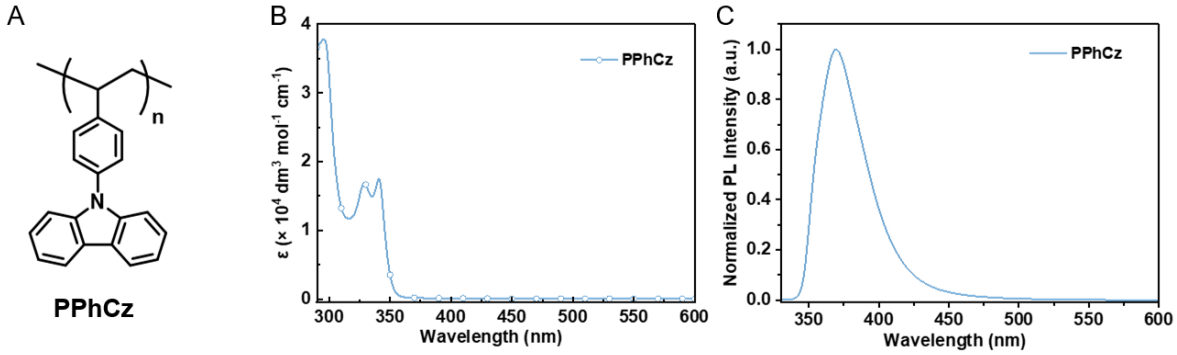

Fig. S8 (A) The chemical structure of homopolymer PPhCz. (B) UV-visible absorption spectra and (B) normalized PL spectra of PPhCz in toluene solution (1×10^{-4} M, 300 K) under 320 nm excitation.

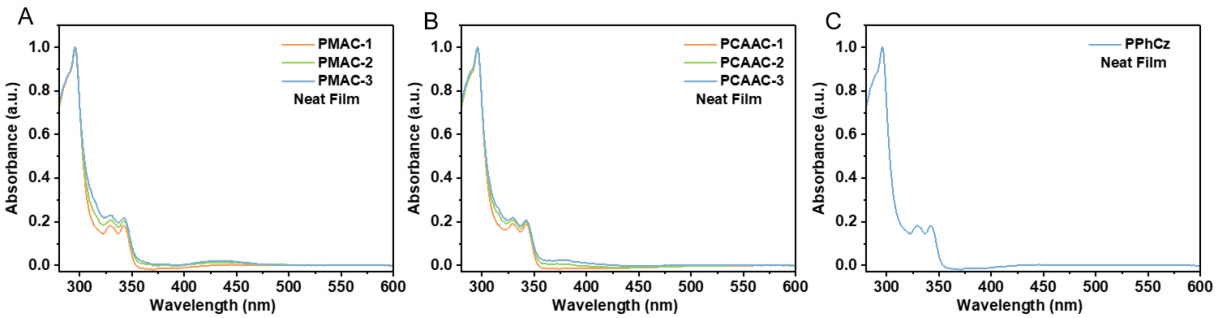

Fig. S9 Normalized absorption spectra of (A) PMAC-x, (B) PCAAC-x, and (C) PPhCz in neat films.

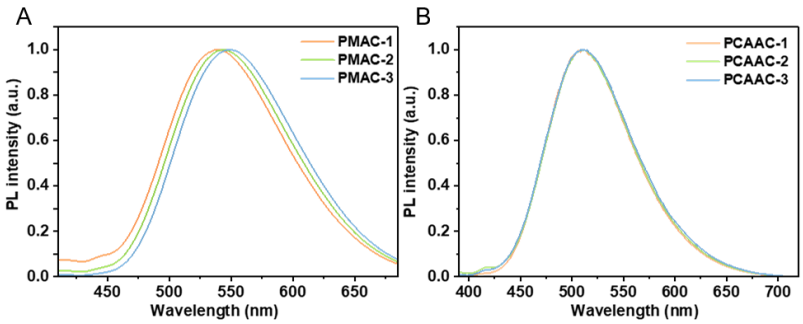

Fig. S10 PL spectra of (A) **PMAC-x** under 400 nm excitation and (B) **PCAAC-x** under 370 nm excitation in toluene solutions (1×10^{-4} M, 300 K).

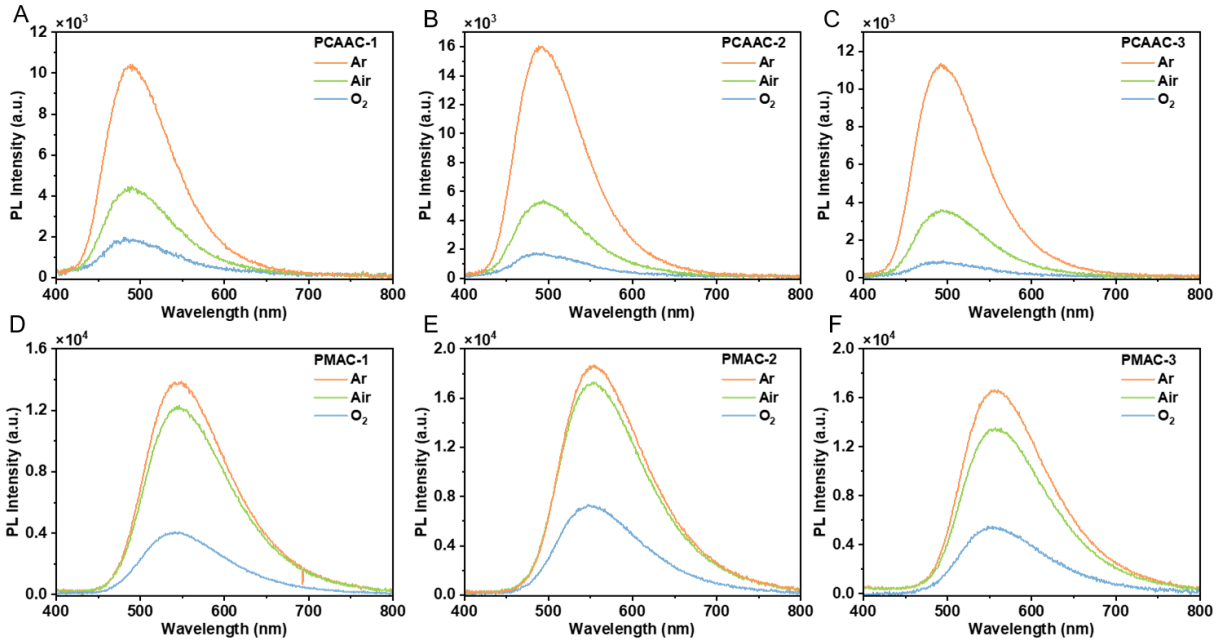

Fig. S11 PL spectra of Cu(I) polymers in neat films measured under Ar, Air and O_2 conditions, following 300 nm excitation.

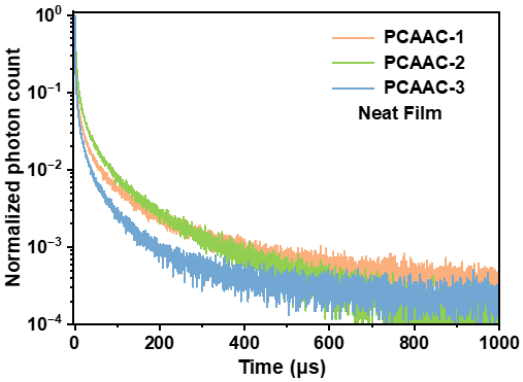

Fig. S12 Transient PL decay curves of **PCAAC-x** in neat films at 300 K, following excitation of 375 nm.

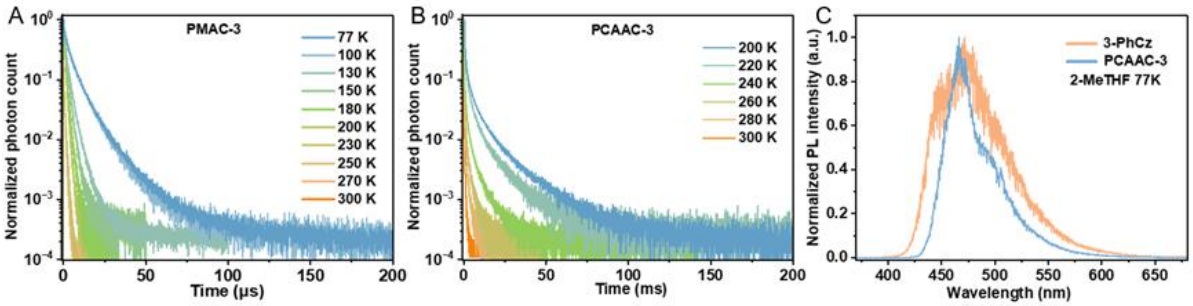

Fig. S13 Transient PL spectra of (A) **PMAC-3** and (B) **PCAAC-3** in neat films from 77 to 300 K, following excitation of 375 nm. (C) Normalized phosphorescence spectra of **PCAAC-3** and 3-PhCz in the 2-MeTHF (10^{-4} M, 77 K), following excitation of 350 nm.

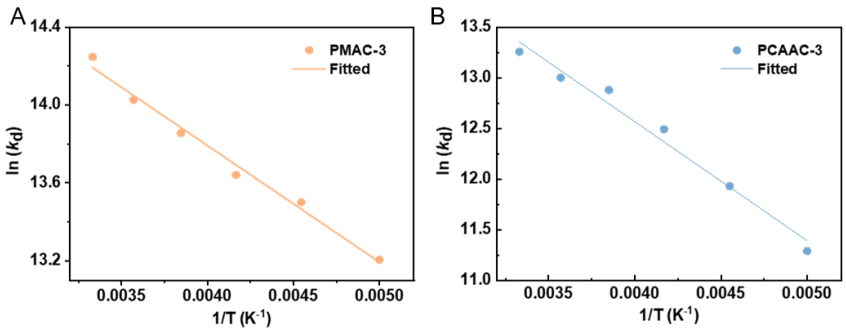

Fig. S14 Fit to the temperature-dependent lifetimes from 200 to 300 K (symbols) to eq. S2 (line) for (A) **PMAC-3** and (B) **PCAAC-3**.

Table S2. Radiative decay lifetimes of **PMAC-3** at different temperatures.

Temperature [K]	τ_1 [ns]	I_1	τ_2 [ns]	I_2	τ_3 [μs]	I_3	τ_{ave} [μs]
77	1540	0.07	8710	0.53	22.8	0.40	13.91
100	1420	0.08	6830	0.62	18.00	0.30	9.81
130	194	0.01	2350	0.42	6.04	0.57	4.42
150	535	0.03	2520	0.53	5.62	0.44	3.81
180	900	0.17	2300	0.75	6.80	0.08	2.43
200	1094	0.44	2371	0.56			1.84
220	897	0.50	1854	0.50			1.37
240	779	0.47	1552	0.53			1.19
260	636	0.45	1128	0.55			0.96
280	502	0.33	959	0.67			0.81
300	380	0.34	797	0.66			0.66

Table S3. Radiative decay lifetimes of **PCAAC-3** at different temperatures.

Temperature [K]	τ_1 [μs]	I_1	τ_2 [μs]	I_2	τ_3 [μs]	I_3	τ_4 [μs]	I_4	τ_{ave} [ms]
77	129	0.03	1530	0.14	7440	0.46	23800	0.37	12.45
100	120	0.03	1280	0.14	6700	0.45	21800	0.38	11.49
120	110	0.04	1140	0.17	6100	0.45	20500	0.34	9.94
140	53	0.05	520	0.13	3700	0.37	15300	0.45	8.28
160	24	0.05	223	0.14	1830	0.29	9990	0.52	5.77
180	22.8	0.06	201	0.18	1600	0.32	9040	0.44	4.54
200	12.5	0.09	105	0.21	746	0.31	4690	0.39	2.10
220	6.59	0.10	47.8	0.24	318	0.33	2127	0.33	0.82
240	3.76	0.12	22.9	0.23	131	0.32	754	0.33	0.30
260	2.55	0.10	12.2	0.24	65.3	0.33	349	0.33	0.14
280	2.26	0.11	12.1	0.24	47.9	0.33	206	0.32	0.08
300	1.75	0.10	7.78	0.27	35.9	0.37	156	0.26	0.05

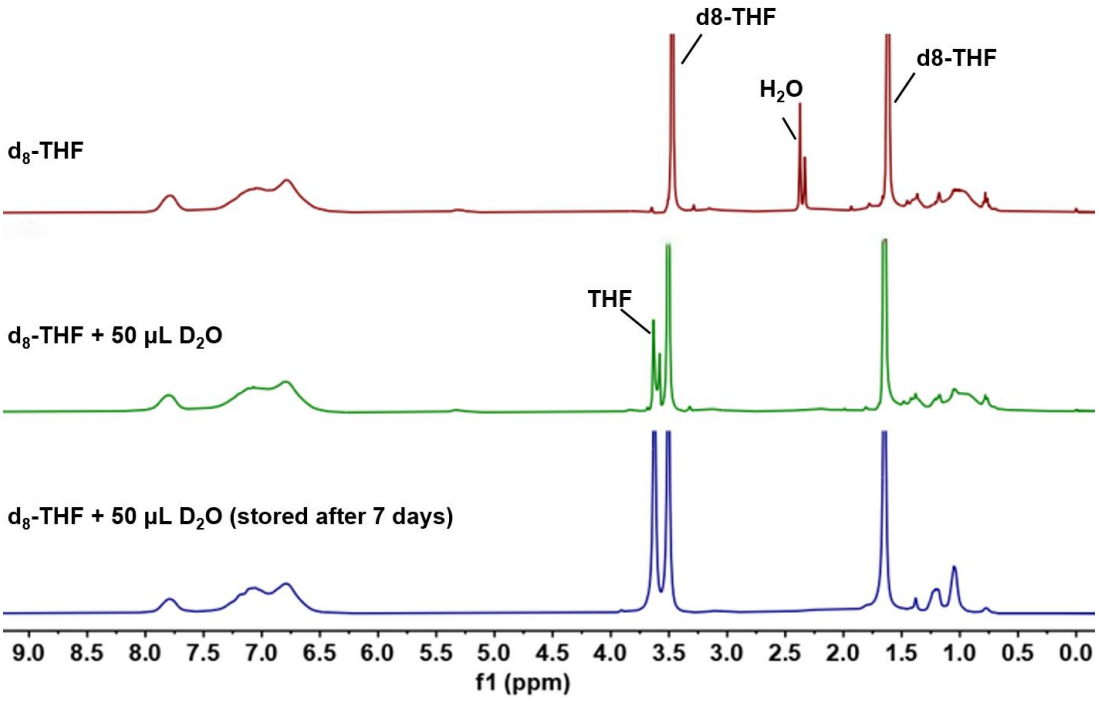

Fig. S15 ^{1}H NMR spectra of **PMAC-3** in the d_8-THF, and the **PMAC-3** with 10% (v: v) D_2O (the volume of the d_8-THF was 0.5 mL) and the sample stored after 7 days.

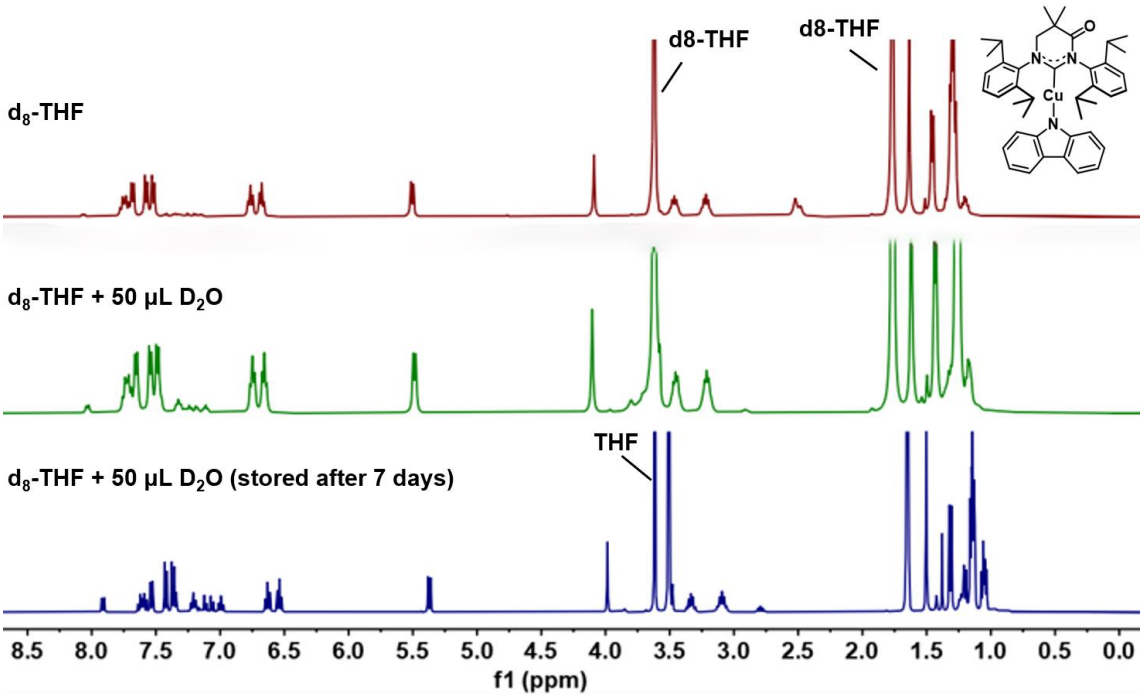

Fig. S16 ^{1}H NMR spectra of MAC-Cu-Cz complex in the d_8-THF, and the MAC-Cu-Cz with 10% (v: v) D_2O (the volume of the d_8-THF was 0.5 mL) and the sample stored after 7 days.

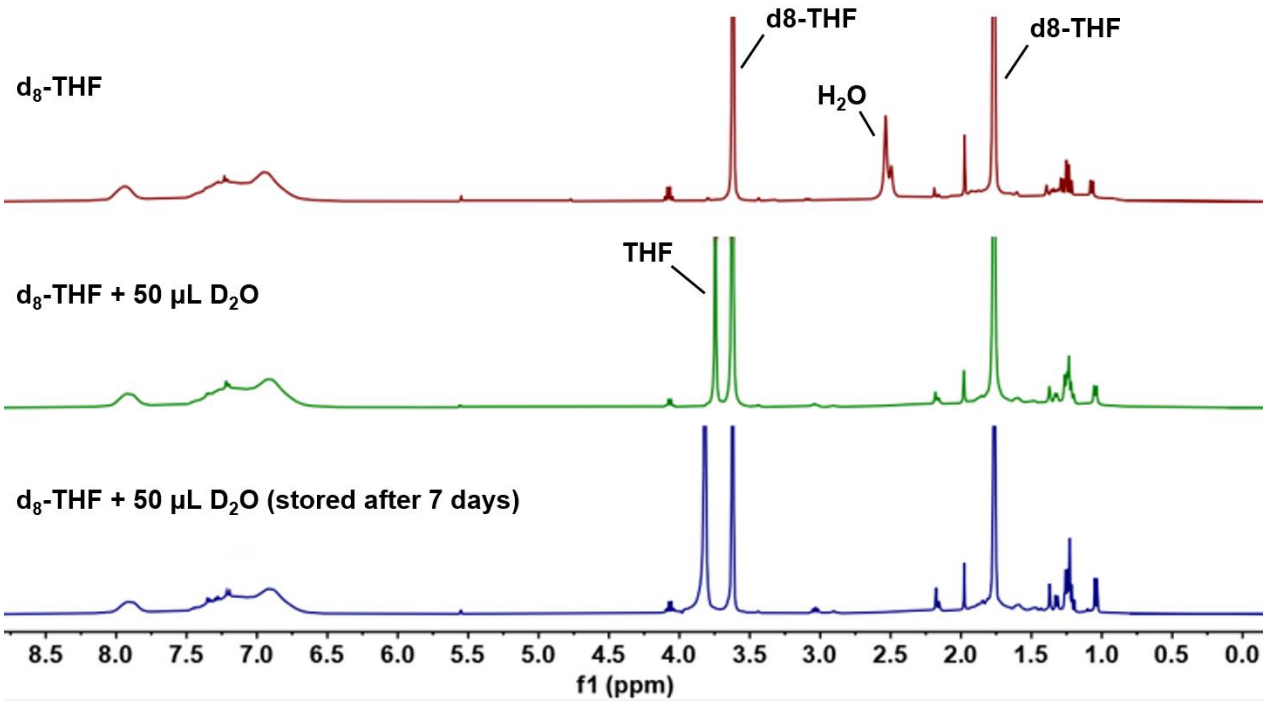

Fig. S17 ^{1}H NMR spectra of **PCAAC-3** in the d_8-THF, and the **PCAAC-3** with 10% (v: v) D_2O (the volume of the d_8-THF was 0.5 mL) and the sample stored after 7 days.

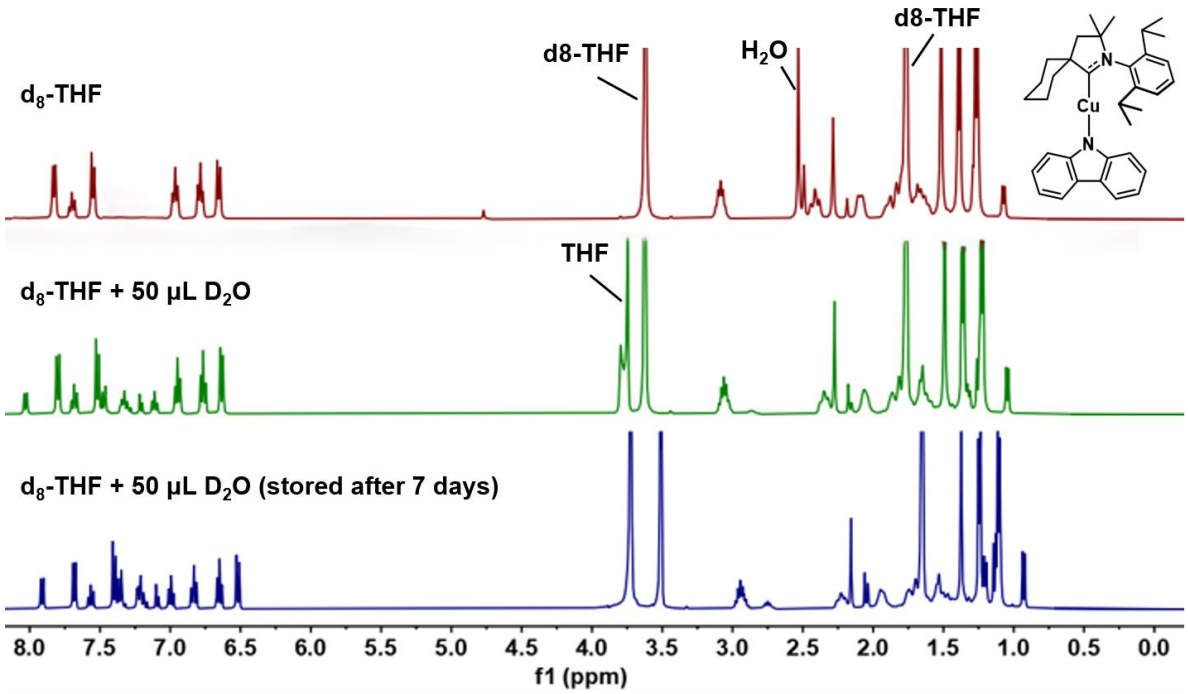

Fig. S18 ^{1}H NMR spectra of CAAC-Cu-Cz complex in the d_8-THF, and the CAAC-Cu-Cz with 10% (v: v) D_2O (the volume of the d_8-THF was 0.5 mL) and the sample stored after 7 days.

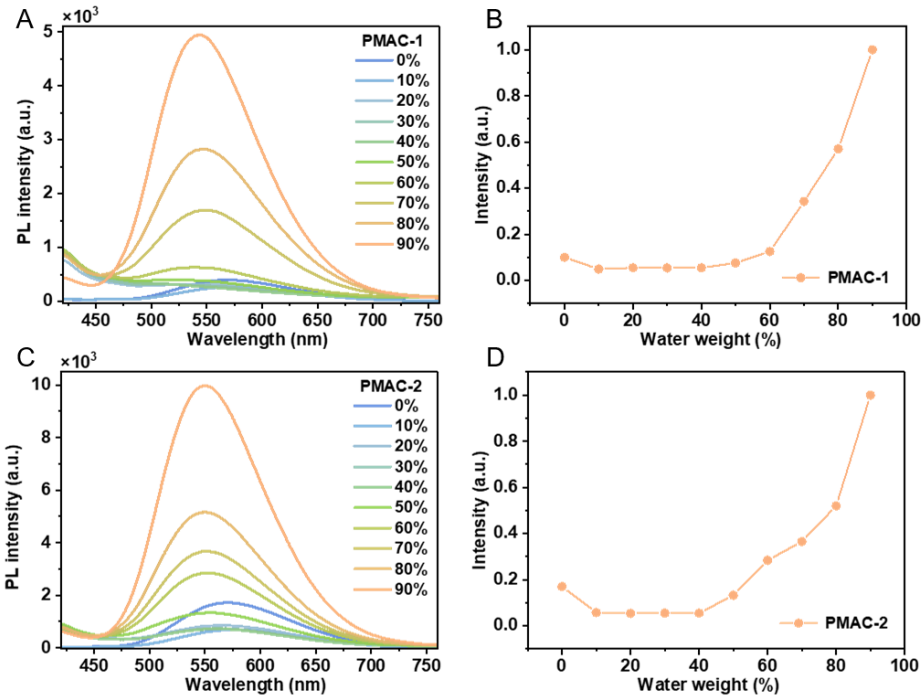

Fig. S19 (A) **PMAC-1** and (C) **PMAC-2** in THF/water mixtures with different water fraction (f_w). Emission intensity vs. f_w of (B) **PMAC-1** and (D) **PMAC-2**.

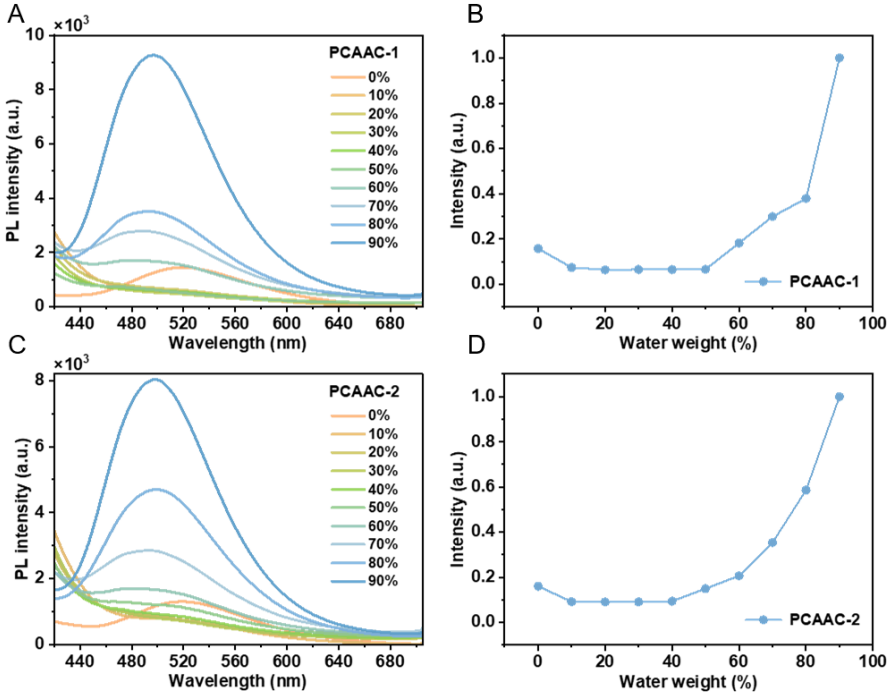

Fig. S20 (A) **PCAAC-1** and (C) **PCAAC-2** in THF/water mixtures with different water fraction (f_w). Emission intensity vs. f_w of (B) **PCAAC-1** and (D) **PCAAC-2**.

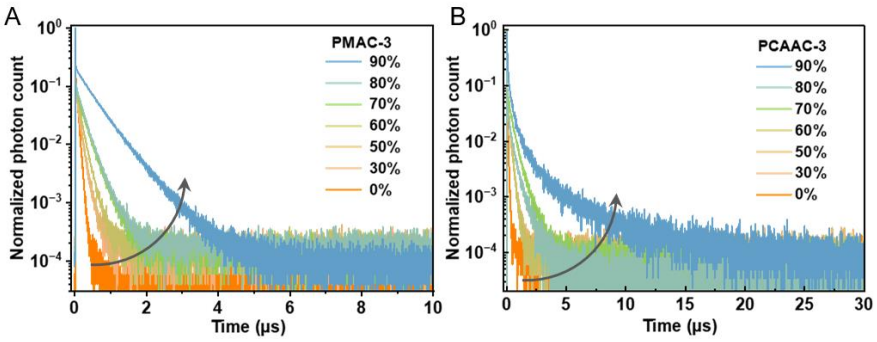

Fig. S21 Normalized transient PL spectra of (A) **PMAC-3** and (B) **PCAAC-3** in the different water fraction (f_w) at 300 K, following excitation of 375 nm.

Table S4. Lifetimes of PMAC-3 and PCAAC-3 in THF/water mixtures with different water fraction.

f_w	lifetime [ns] $_{@PMAC-3}$	lifetime [μs] $_{@PMAC-3}$
0%	54	0.05
30%	105	0.13
50%	137	0.19
60%	143	0.25
70%	225	0.48
80%	253	1.12
90%	508	2.70

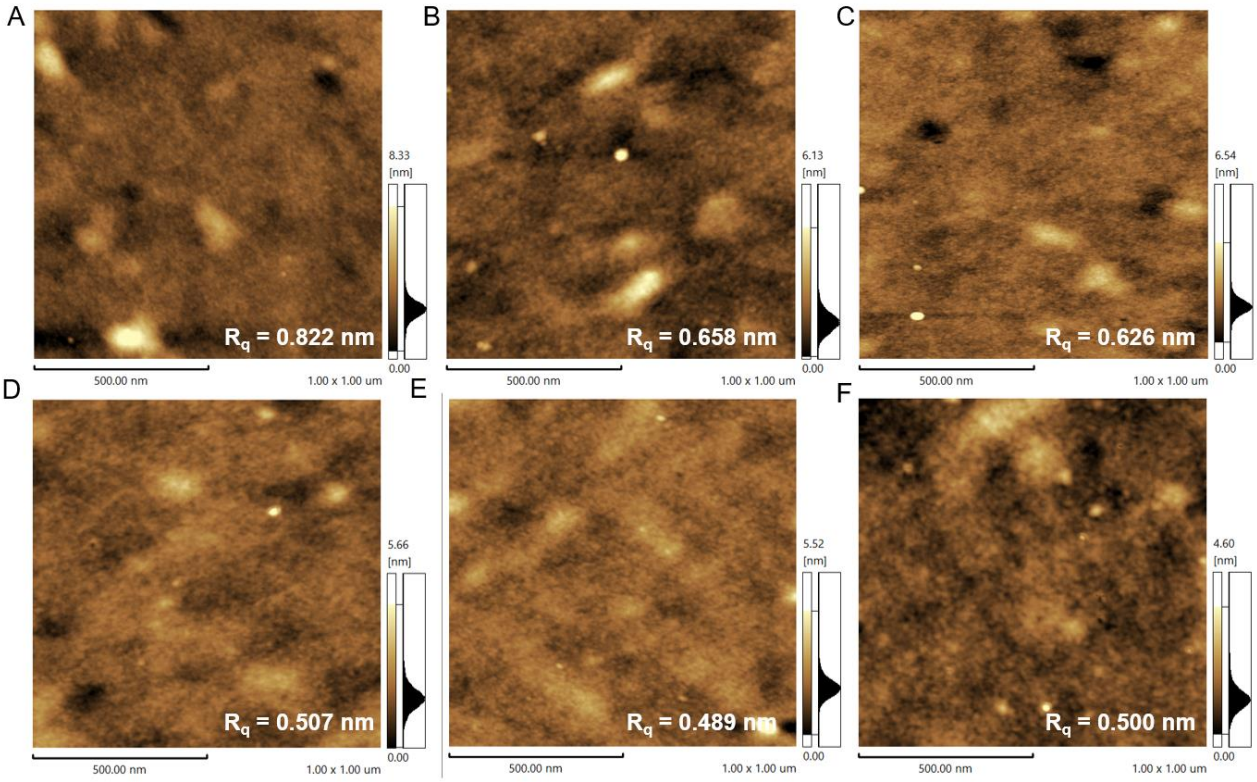

Fig. S22 Atom force microscopy (AFM) images of neat films for (A) **PMAC-1**, (B) **PMAC-2**, (C) **PMAC-3**, (D) **PCAAC-1**, (E) **PCAAC-2** and (F) **PCAAC-3**.

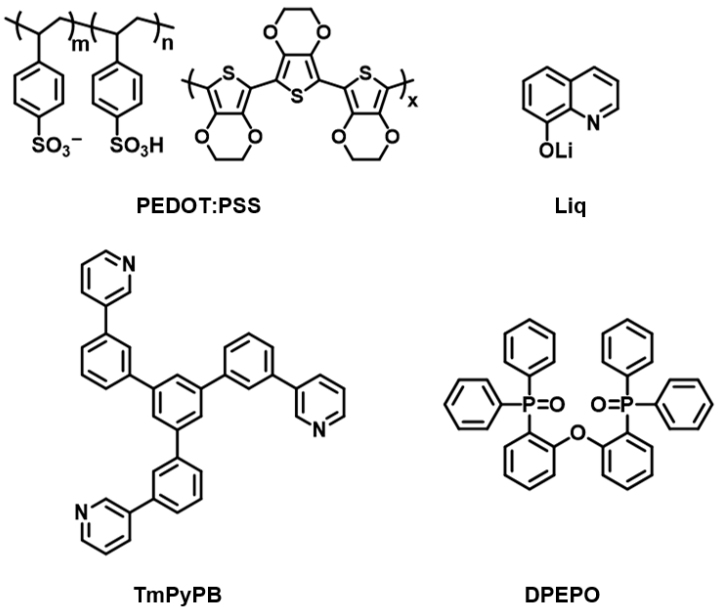

Fig. S23 Molecular structures of the materials used in the devices.

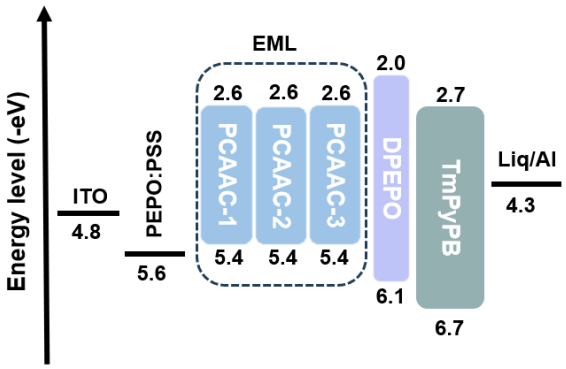

Fig. S24 Device structure and energy level diagram of device 4-6.

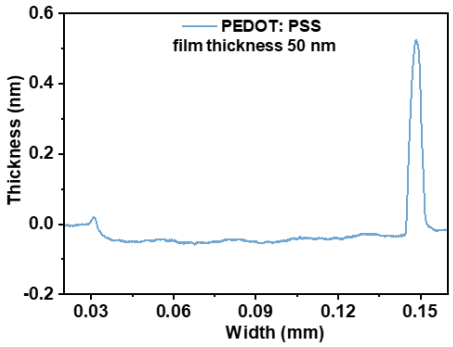

Fig. S25 The thickness of hole-injection layer (PEDOT: PSS).

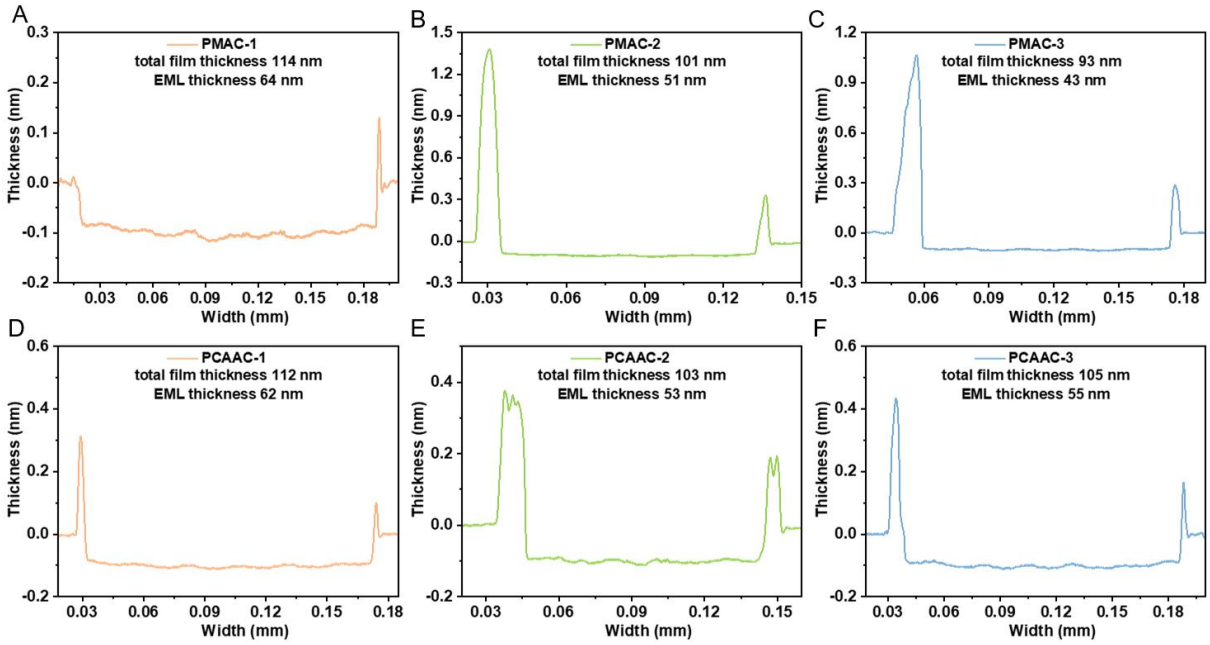

Fig. S26 The thickness of the emissive layers based on all the Cu(I) polymers.

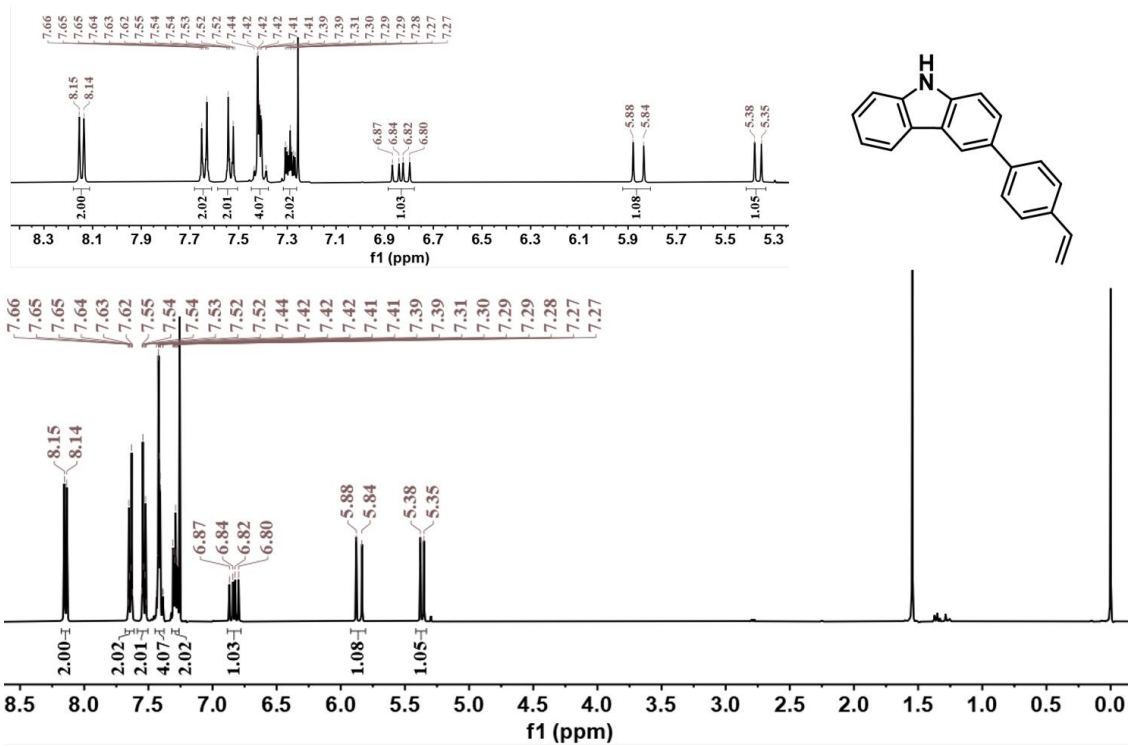

Fig. S27 ^{1}H NMR spectrum of 3-(4-vinylphenyl)-9*H*-carbazole (400 MHz, $CDCl_3$ + TMS, 300 K).

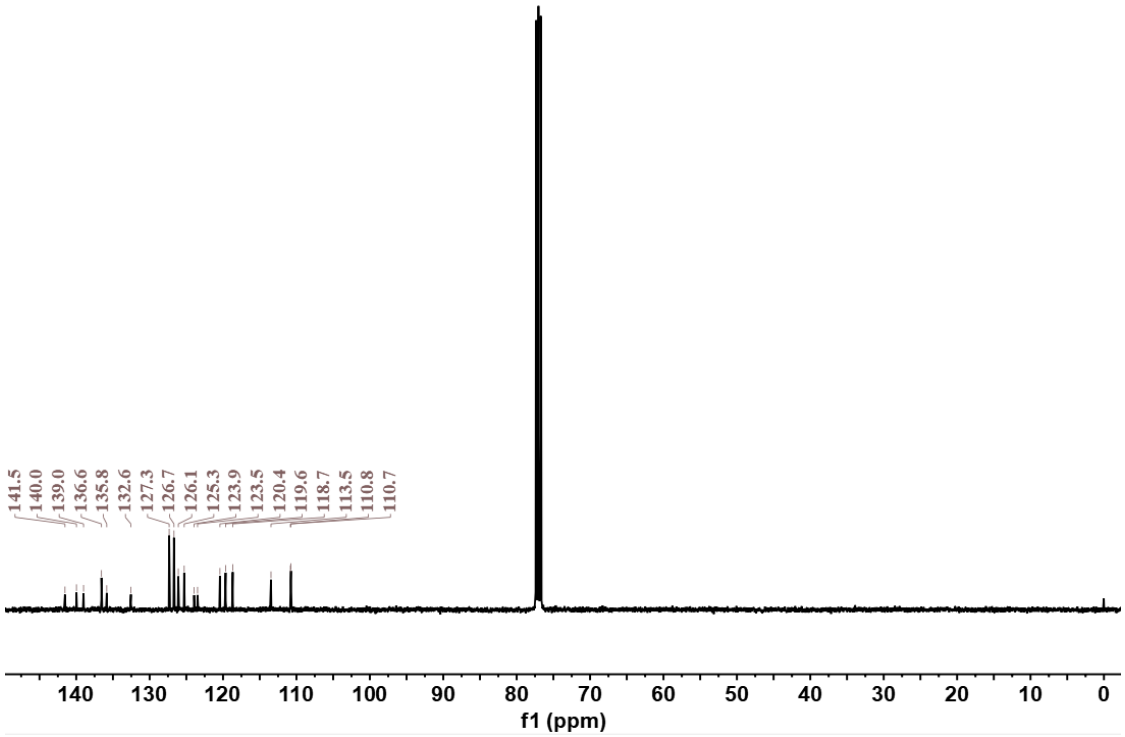

Fig. S28 ^{13}C NMR spectrum of 3-(4-vinylphenyl)-9*H*-carbazole (101 MHz, $CDCl_3$ + TMS, 300 K).

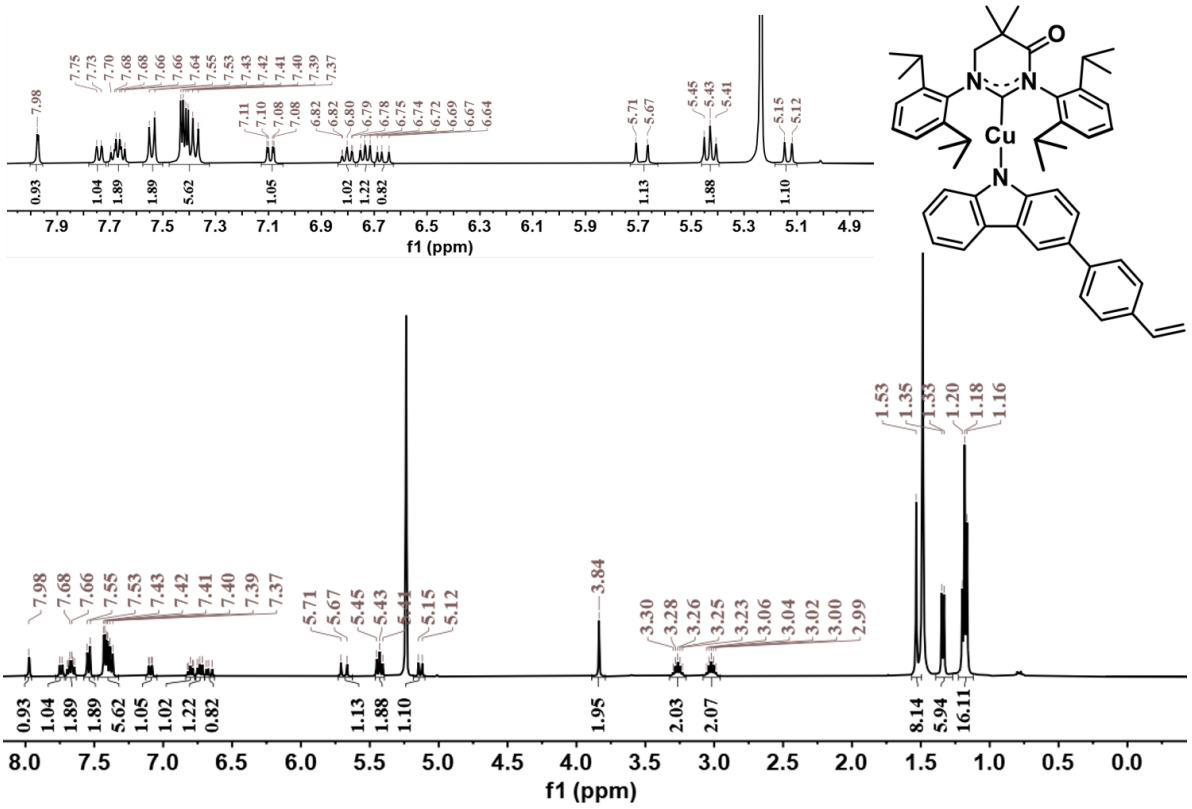

Fig. S29 ^{1}H NMR spectrum of MAC-Cu-PhCz monomer (400 MHz, CD_2Cl_2 + TMS, 300 K).

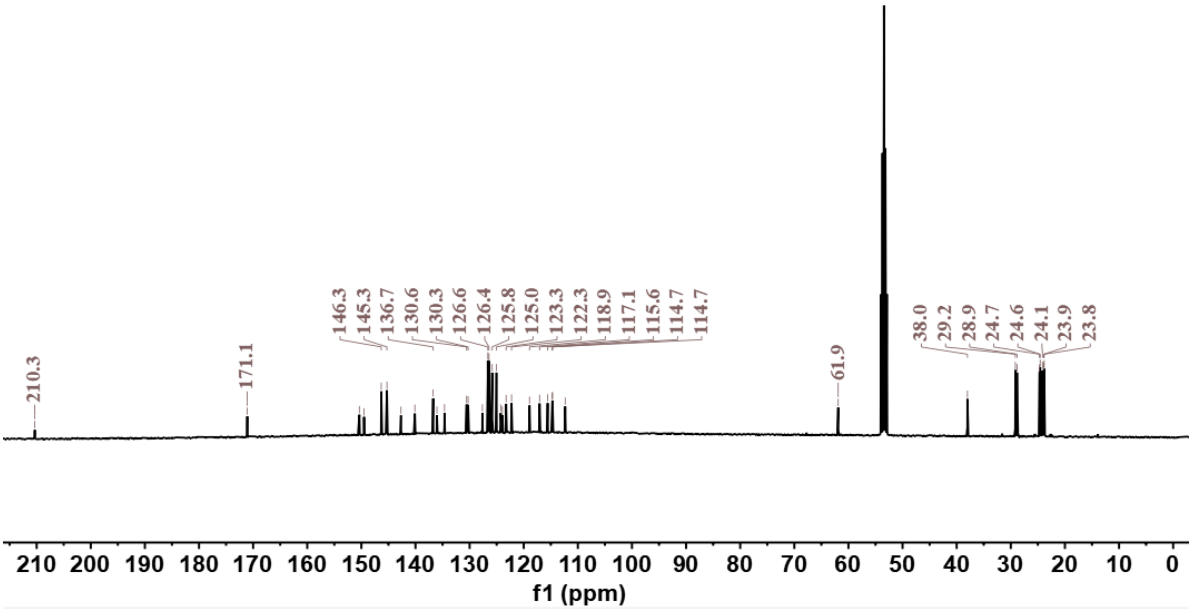

Fig. S30 ^{13}C NMR spectrum of MAC-Cu-PhCz monomer (101 MHz, CD_2Cl_2 + TMS, 300 K).

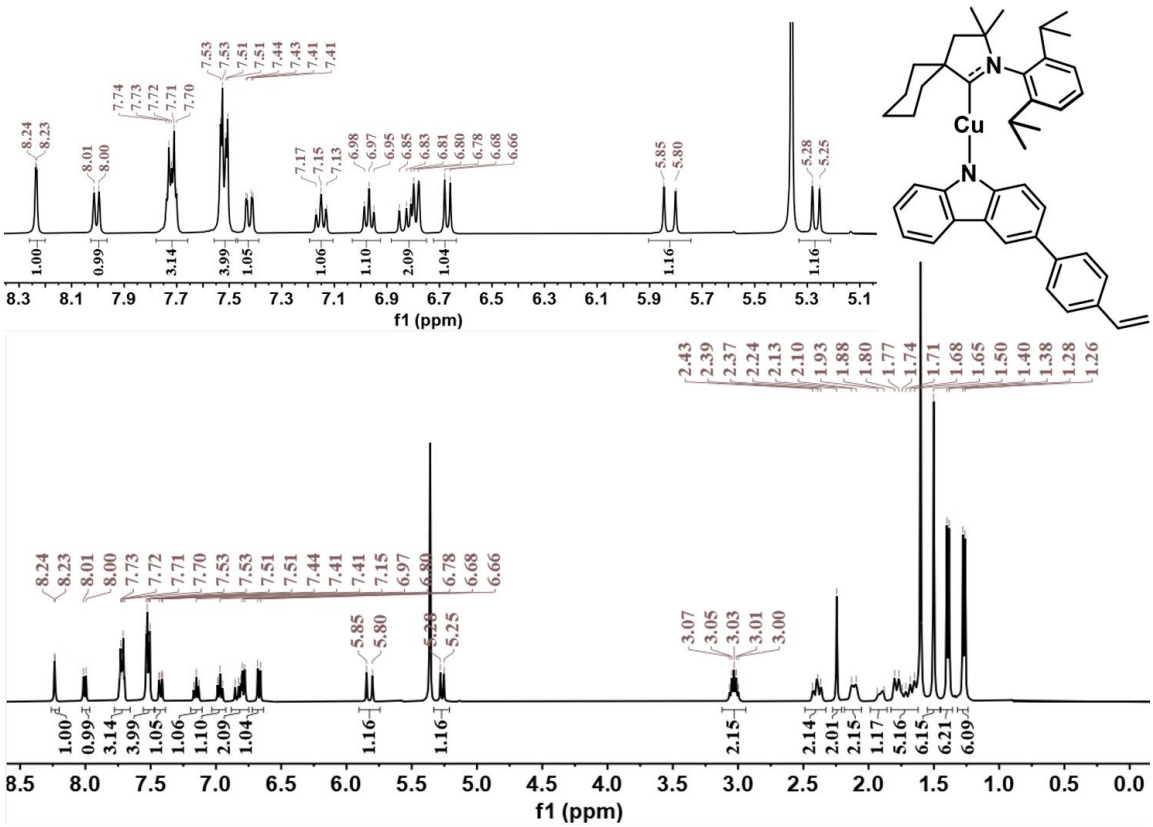

Fig. S31 ^{1}H NMR spectrum of CAAC-Cu-PhCz monomer (400 MHz, CD_2Cl_2 + TMS, 300 K).

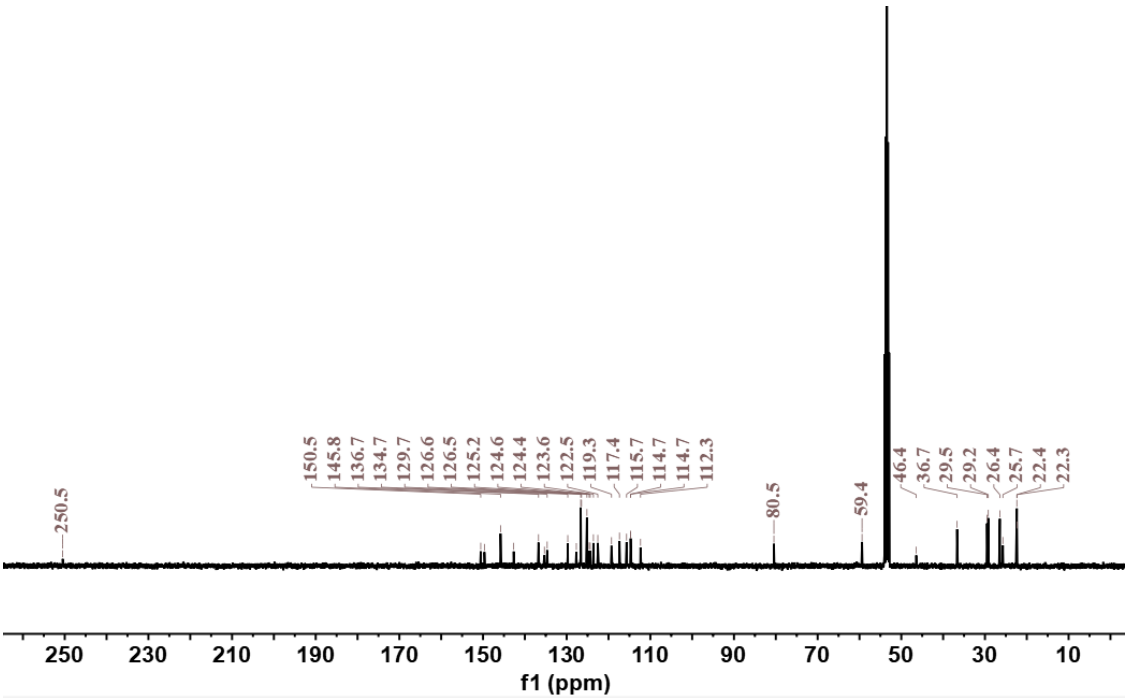

Fig. S32 ^{13}C NMR spectrum of CAAC-Cu-PhCz monomer (101 MHz, CD_2Cl_2 + TMS, 300 K).

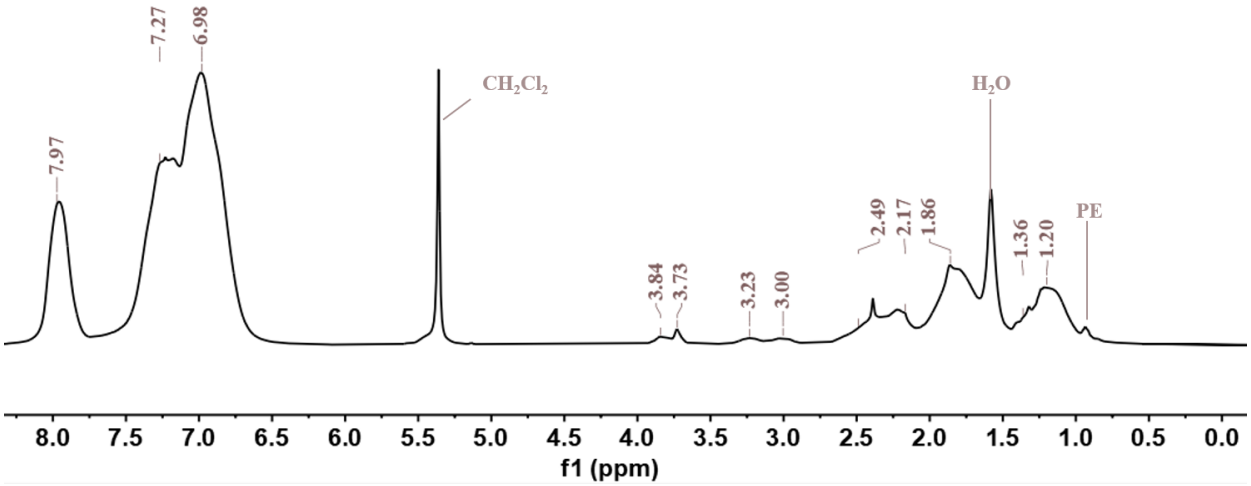

Fig. S33 ^{1}H NMR spectrum of **PMAC-1** (400 MHz, CD_2Cl_2 + TMS, 300 K).

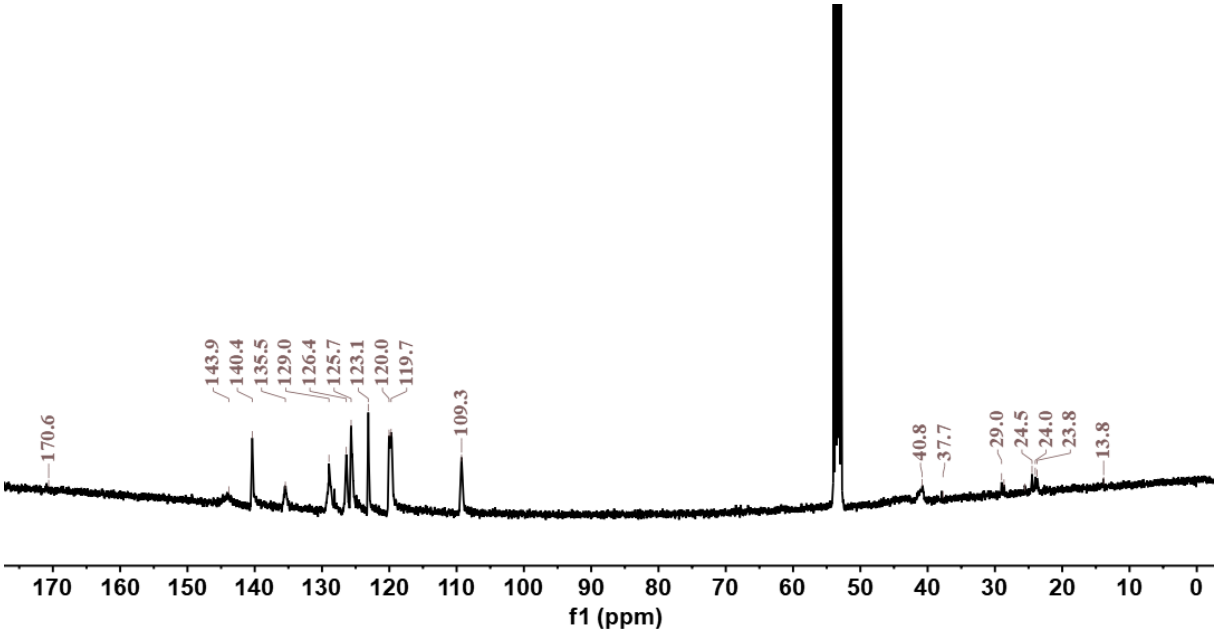

Fig. S34 ^{13}C NMR spectrum of **PMAC-1** (101 MHz, CD_2Cl_2 + TMS, 300 K).

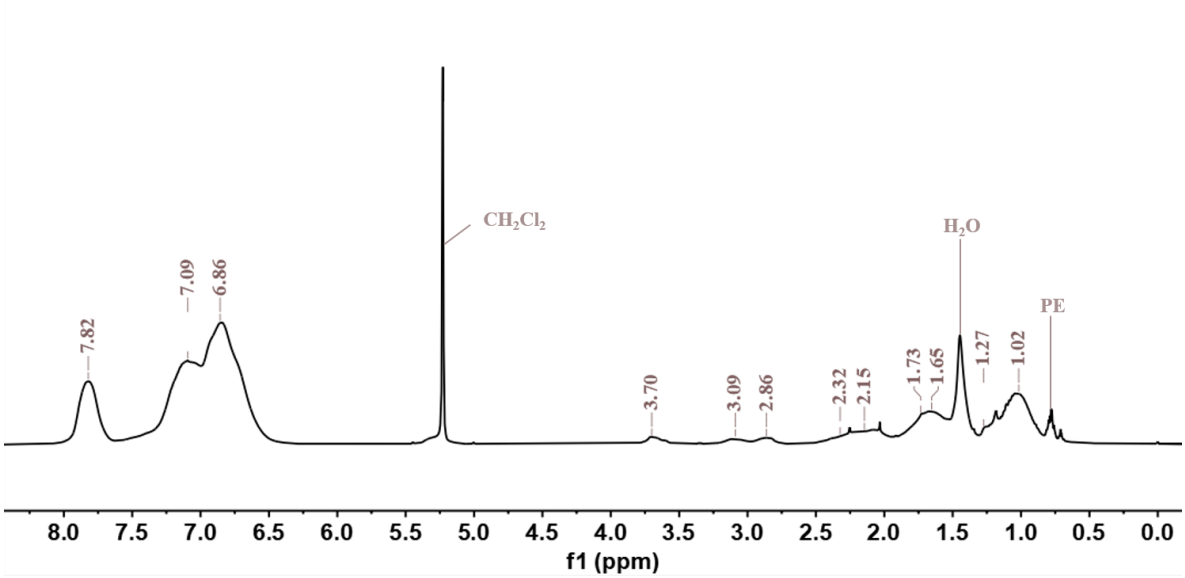

Fig. S35 ^{1}H NMR spectrum of **PMAC-2** (400 MHz, CD_2Cl_2 + TMS, 300 K).

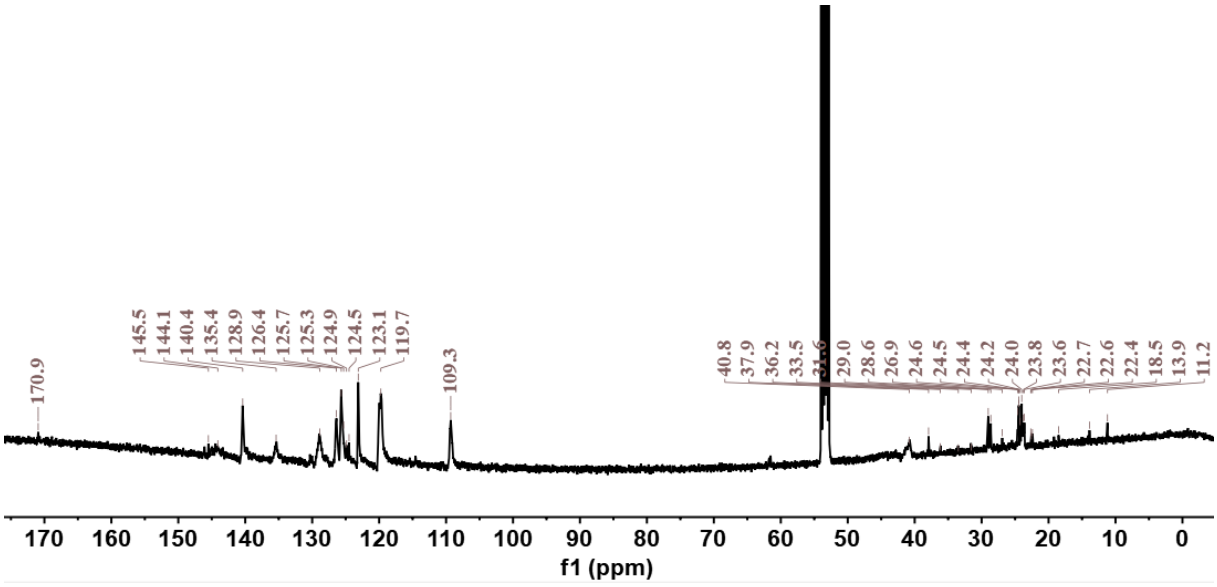

Fig. S36 ^{13}C NMR spectrum of **PMAC-2** (101 MHz, CD_2Cl_2 + TMS, 300 K).

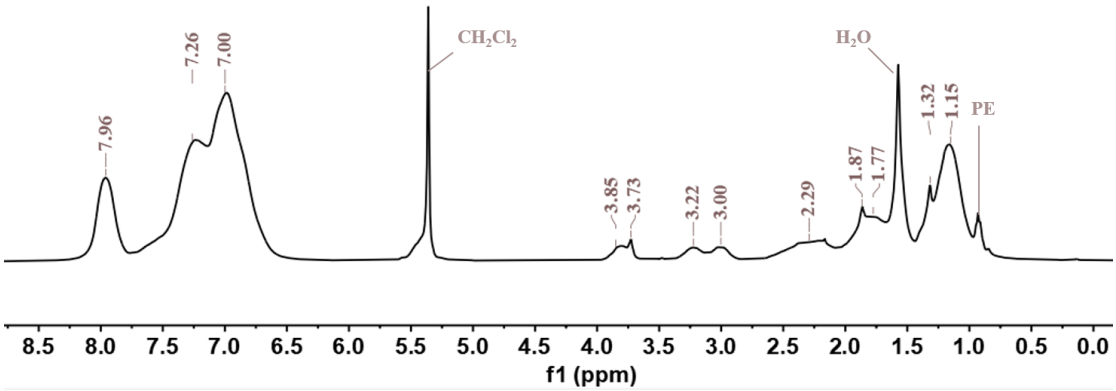

Fig. S37 ^{1}H NMR spectrum of **PMAC-3** (400 MHz, CD_2Cl_2 + TMS, 300 K).

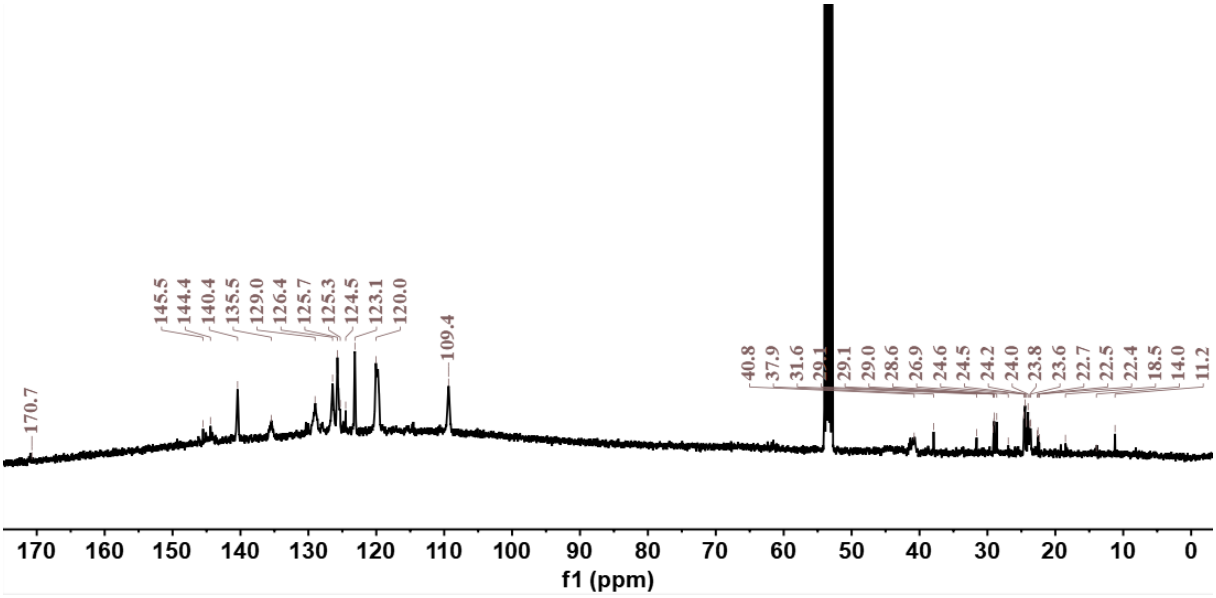

Fig. S38 ^{13}C NMR spectrum of **PMAC-3** (101 MHz, CD_2Cl_2 + TMS, 300 K).

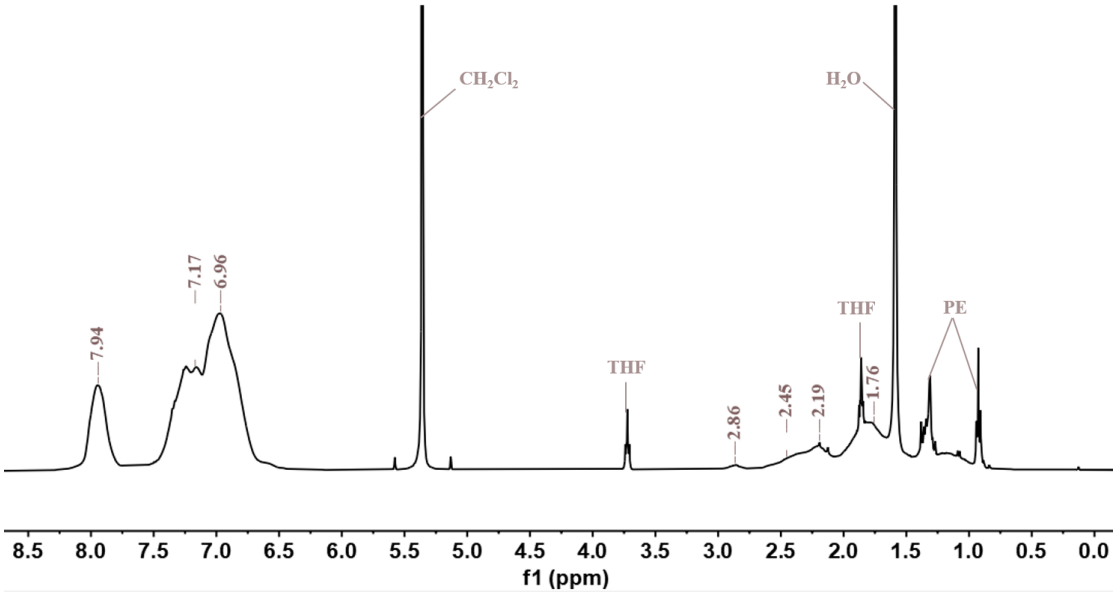

Fig. S39 ^{1}H NMR spectrum of **PCAAC-1** (400 MHz, CD_2Cl_2 + TMS, 300 K).

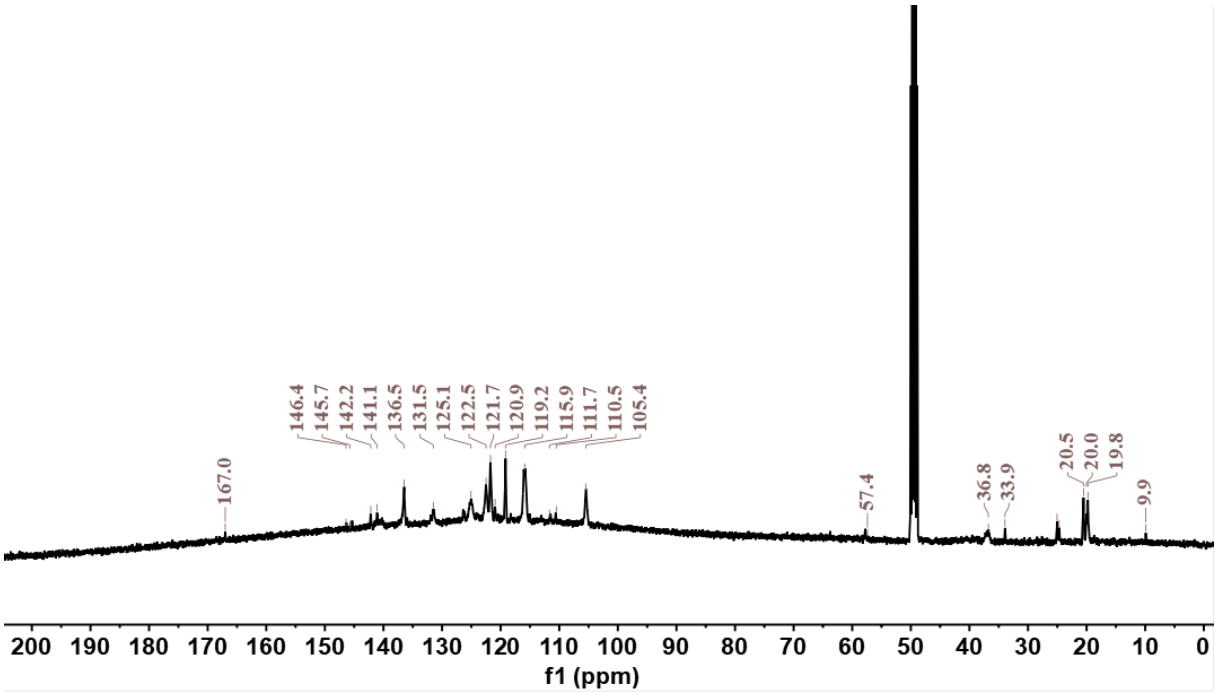

Fig. S40 ^{13}C NMR spectrum of **PCAAC-1** (101 MHz, CD_2Cl_2 + TMS, 300 K).

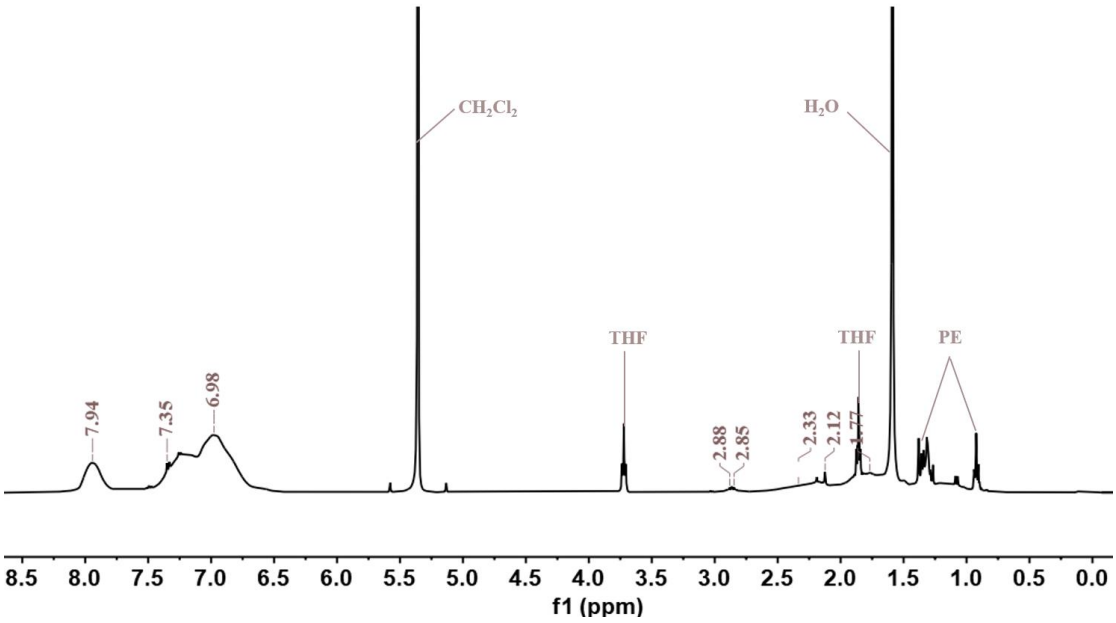

Fig. S41 ^{1}H NMR spectrum of **PCAAC-2** (400 MHz, CD_2Cl_2 + TMS, 300 K).

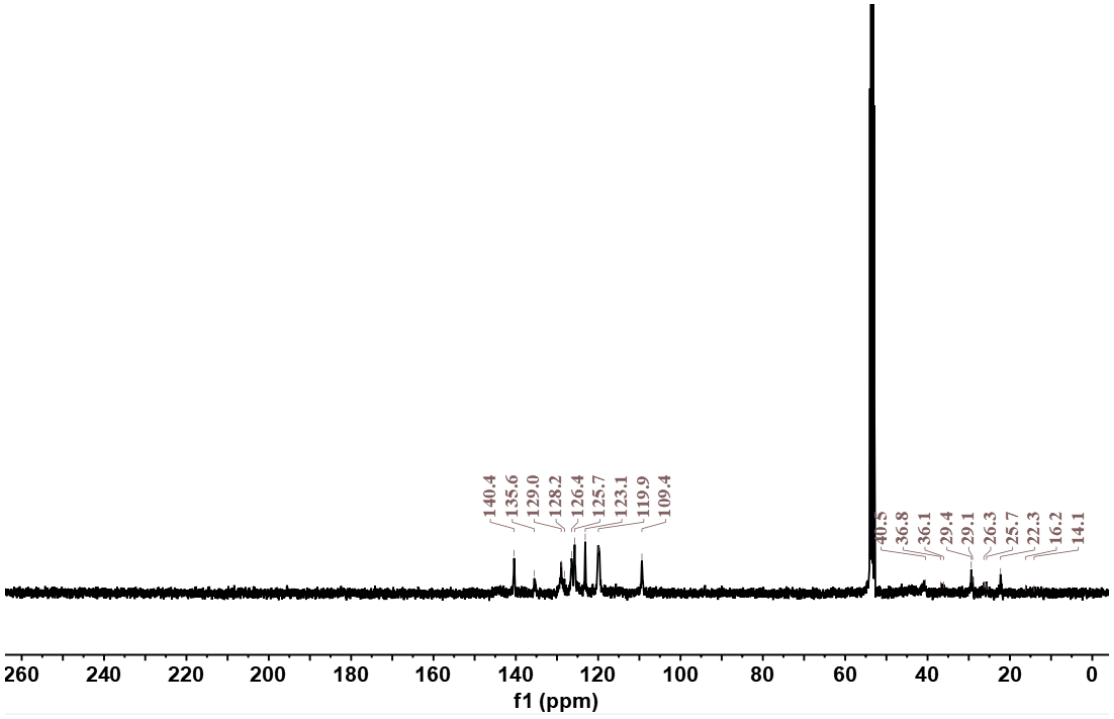

Fig. S42 ^{13}C NMR spectrum of **PCAAC-2** (101 MHz, CD_2Cl_2+ TMS, 300 K).

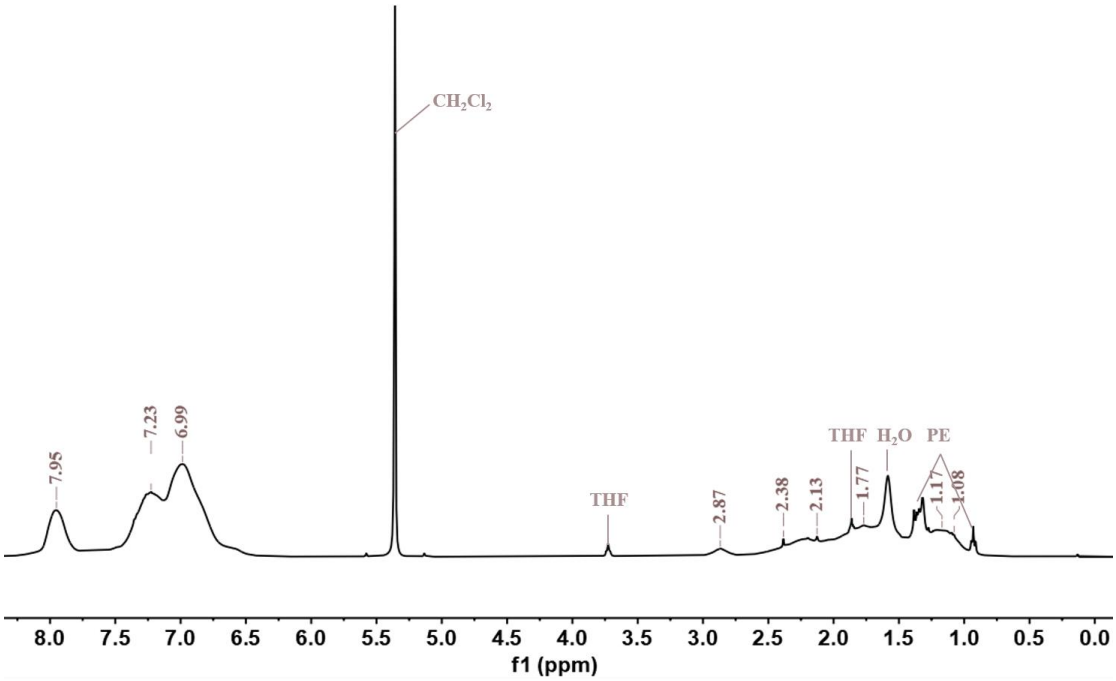

Fig. S43 ^{1}H NMR spectrum of **PCAAC-3** (400 MHz, CD_2Cl_2+ TMS, 300 K).

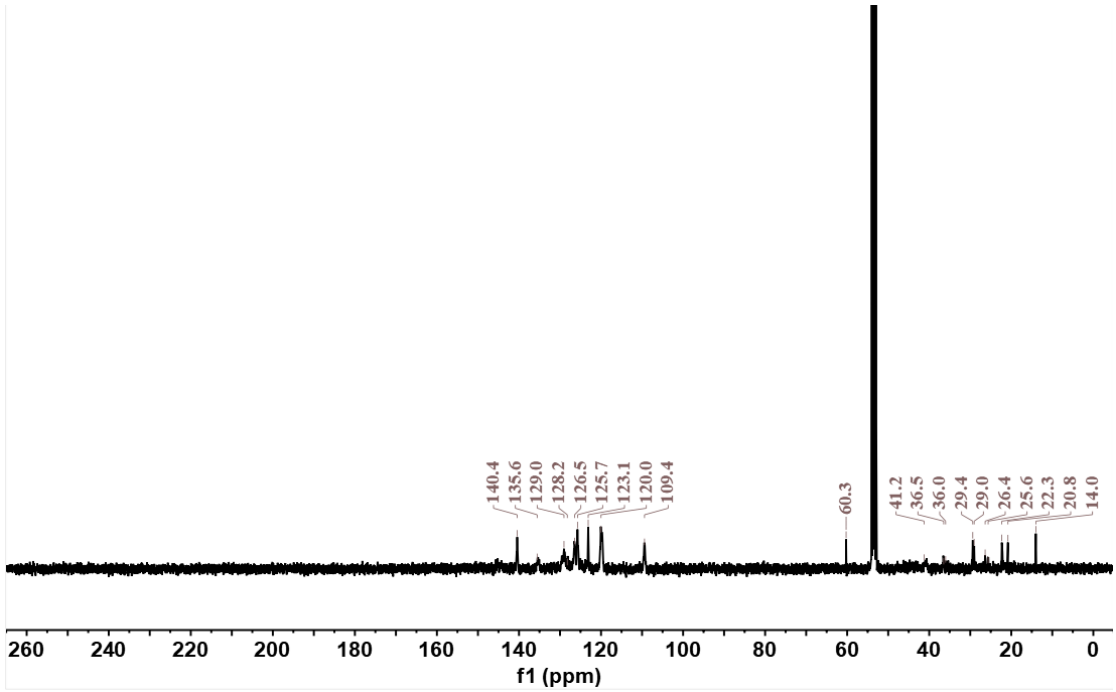

Fig. S44 ^{13}C NMR spectrum of **PCAAC-3** (101 MHz, CD_2Cl_2 + TMS, 300 K).

References

1. S. Grimme, S. Ehrlich and L. Goerigk, *J. Comput. Chem*., 2011, **32**, 1456–1465.
2. S. Grimme, J. Antony, S. Ehrlich and H. Krieg, *J. Chem. Phys*., 2010, **132**, 154104.
3. T. Lu and F. Chen, *J. Comput. Chem.*, 2011, **33**, 580–592.
4. R. Hamze, S. Shi, S. C. Kapper, D. S. Muthiah Ravinson, L. Estergreen, M.-C. Jung, A. C. Tadle, R. Haiges, P. I. Djurovich, J. L. Peltier, R. Jazzar, G. Bertrand, S. E. Bradforth and M. E. Thompson, *J. Am. Chem. Soc*., 2019, **141**, 8616–8626.
5. G. D. Frey, R. D. Dewhurst, S. Kousar, B. Donnadieu, G. Bertrand, *J. Organometal. Chem.* 2008, **693**, 1674–1682
6. S. Shi, M. C. Jung, C. Coburn, A. Tadle, D. Sylvinson M. R, P. I. Djurovich, S. R. Forrest, M. E. Thompson, J. *Am. Chem. Soc.* 2019, **141**, 3576–3588.